Supporting Information For

Suppressing lattice distortion *via* engineering oxygen vacancy into sub-5 nm NiO for durable methanol electrooxidation

Tao Chen,*[1,2,4], Zhiying Lyu [3], Jiaxing Song*[2]

1 State Key Laboratory of Silicon and Advanced Semiconductor Materials, Department of Polymer Science and Engineering, Zhejiang University, Hangzhou 310027, PR China.

2 Zhejiang Key Laboratory of Advanced Tandem Photovoltaic Technology, College of Biological and Chemical Engineering, Jiaxing University, Jiaxing 314001, PR China.

3 RWTH International Academy, RWTH Aachen University, Aachen, 52074, Germany.

4 G60 STI Valley Industry & Innovation Institute Jiaxing University, Jiaxing 314001, PR China.

Corresponding Authors

E-mail: 0624528@zju.edu.cn; songjx@zjxu.edu.cn

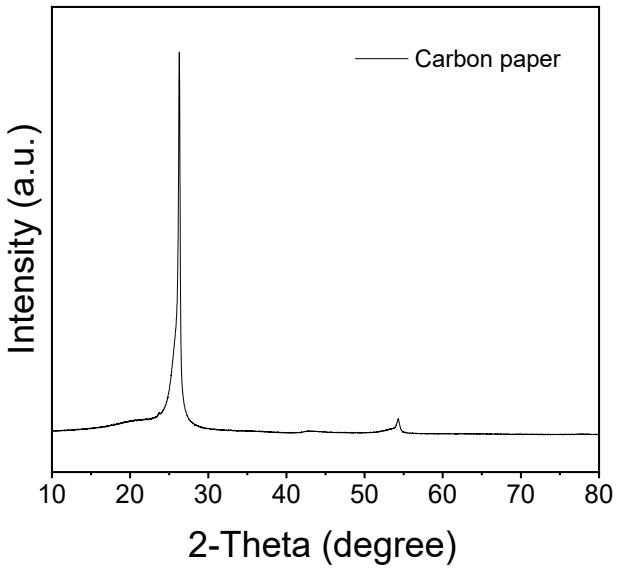

Supplementary Fig. 1 XRD pattern of carbon paper.

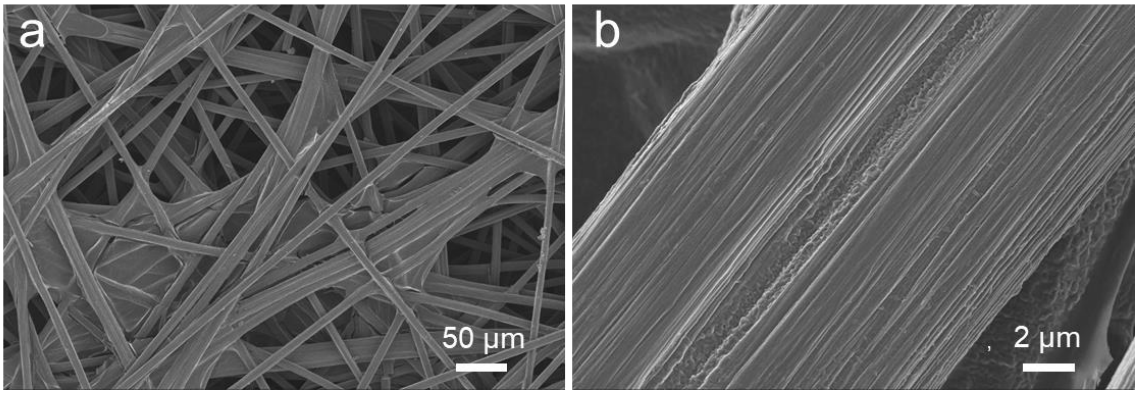

Supplementary Fig. 2 SEM images of carbon paper.

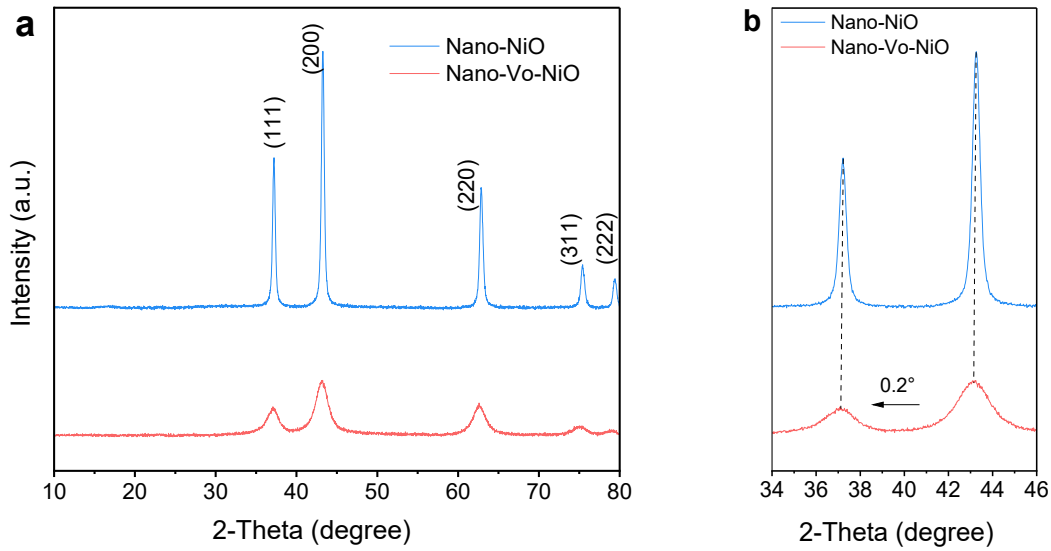

Supplementary Fig. 3 a XRD patterns of Nano-NiO and Nano-Vo-NiO. **b** Amplified region of the 2θ range from 34° to 46°

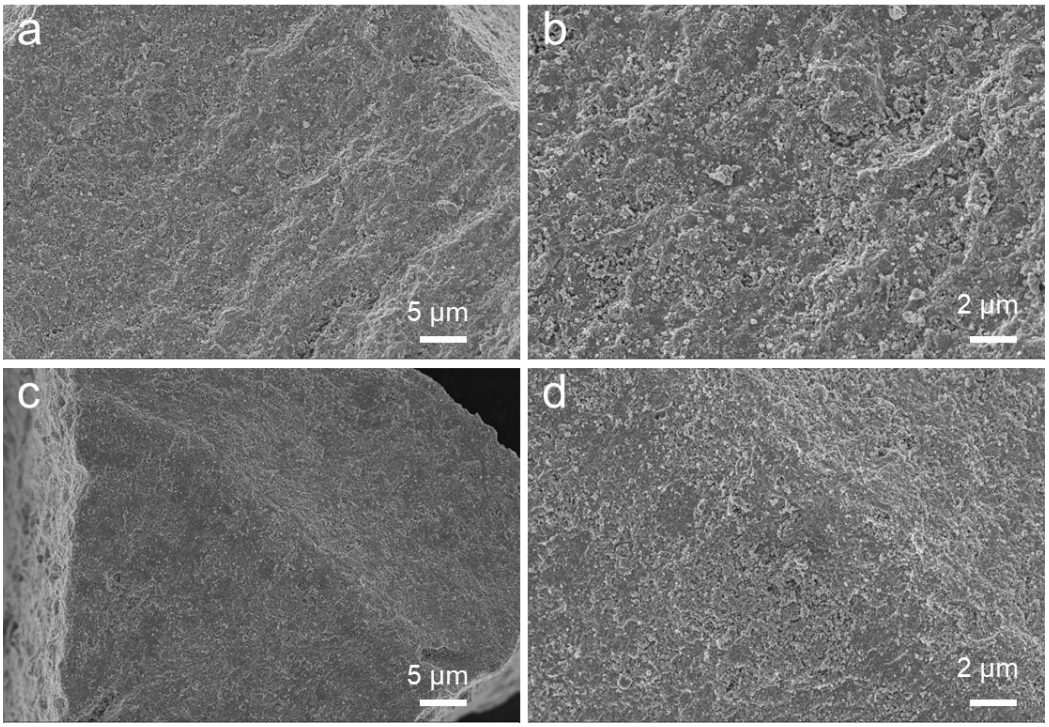

Supplementary Fig. 4 SEM images of **a,b** Nano-NiO and **c,d** Nano-Vo-NiO.

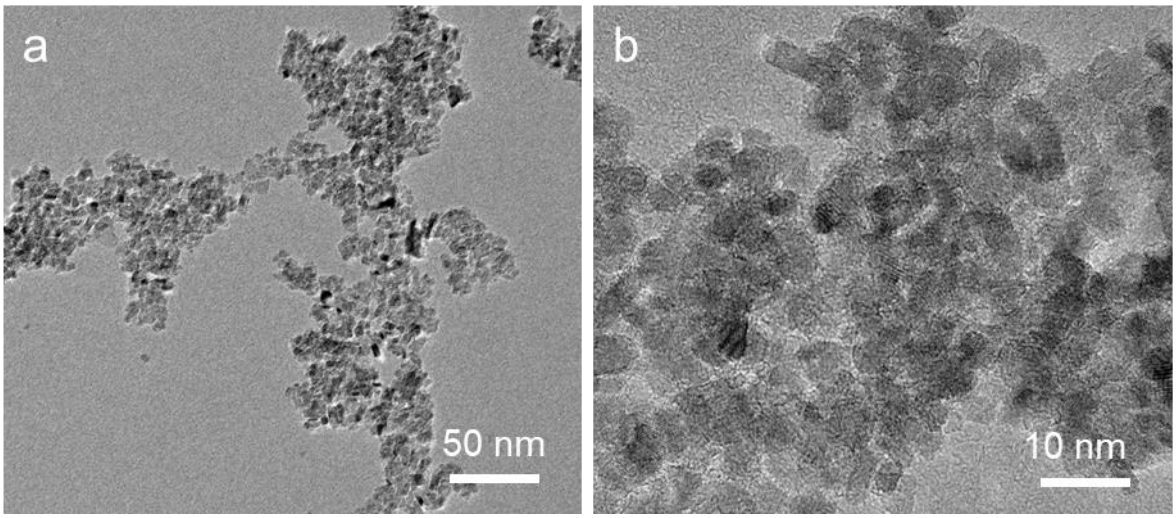

Supplementary Fig. 5 HR-TEM images of Nano-Vo-NiO.

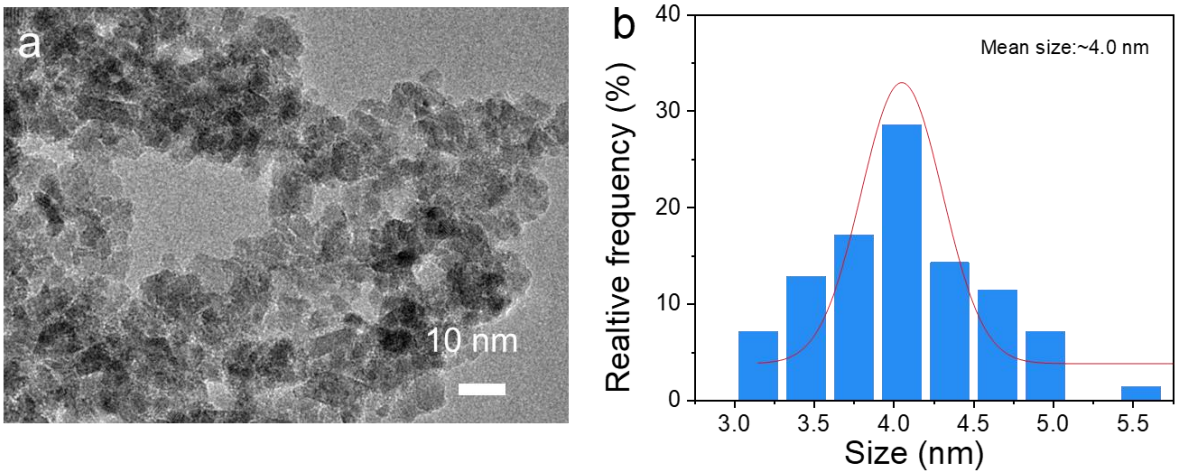

Supplementary Fig. 6 a HR-TEM image and **b** the particle size distributions on Nano-NiO.

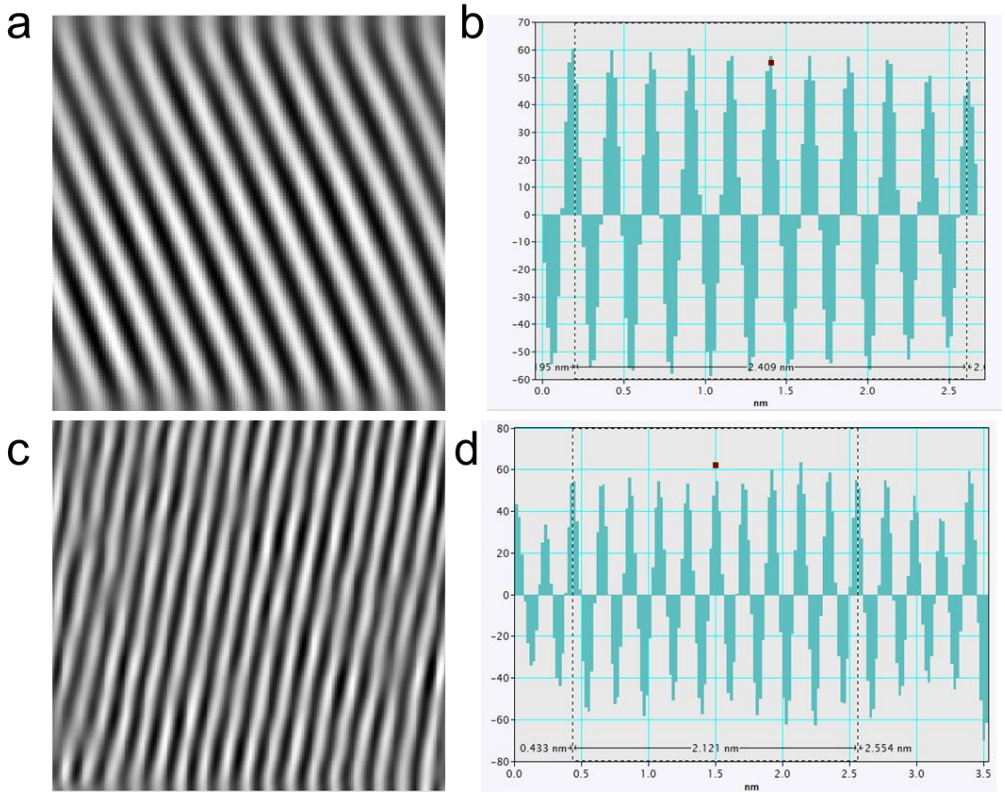

Supplementary Fig. 7 a,c Fourier-filtered image and **b,d** corresponding line intensity profiles for (111) and (200) crystal planes of Nano-Vo-NiO.

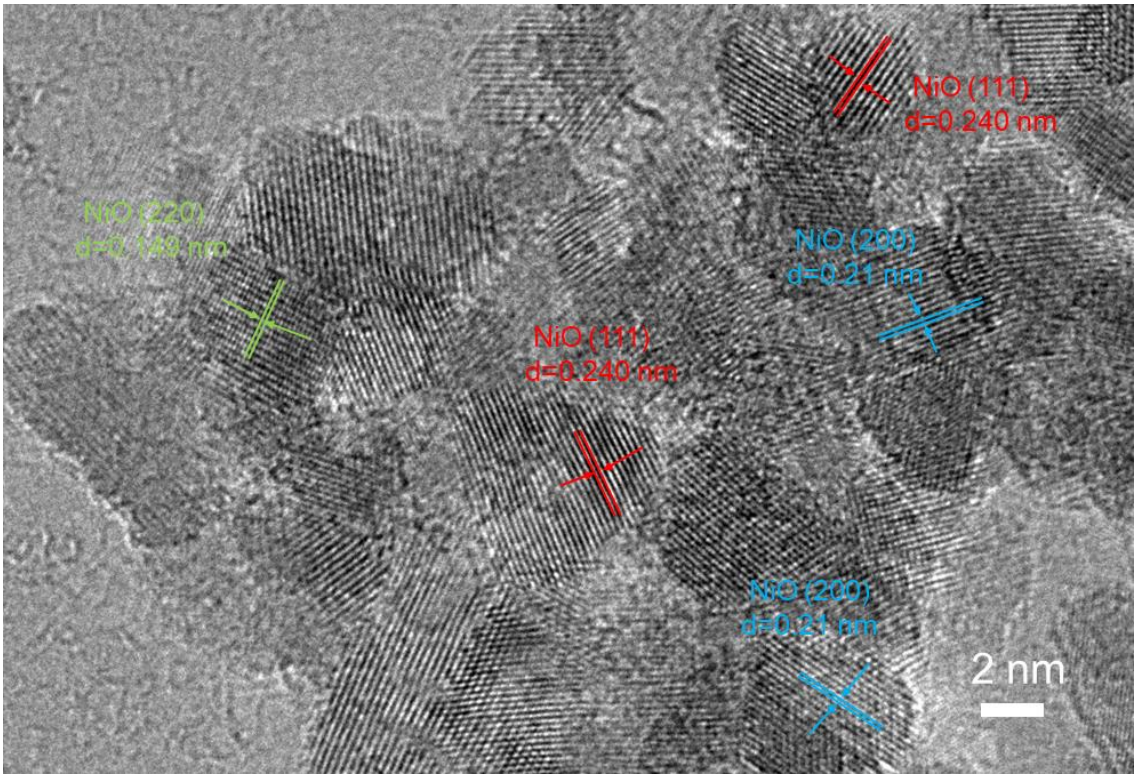

Supplementary Fig. 8 HR-TEM images with clear lattice fringes of Nano-NiO.

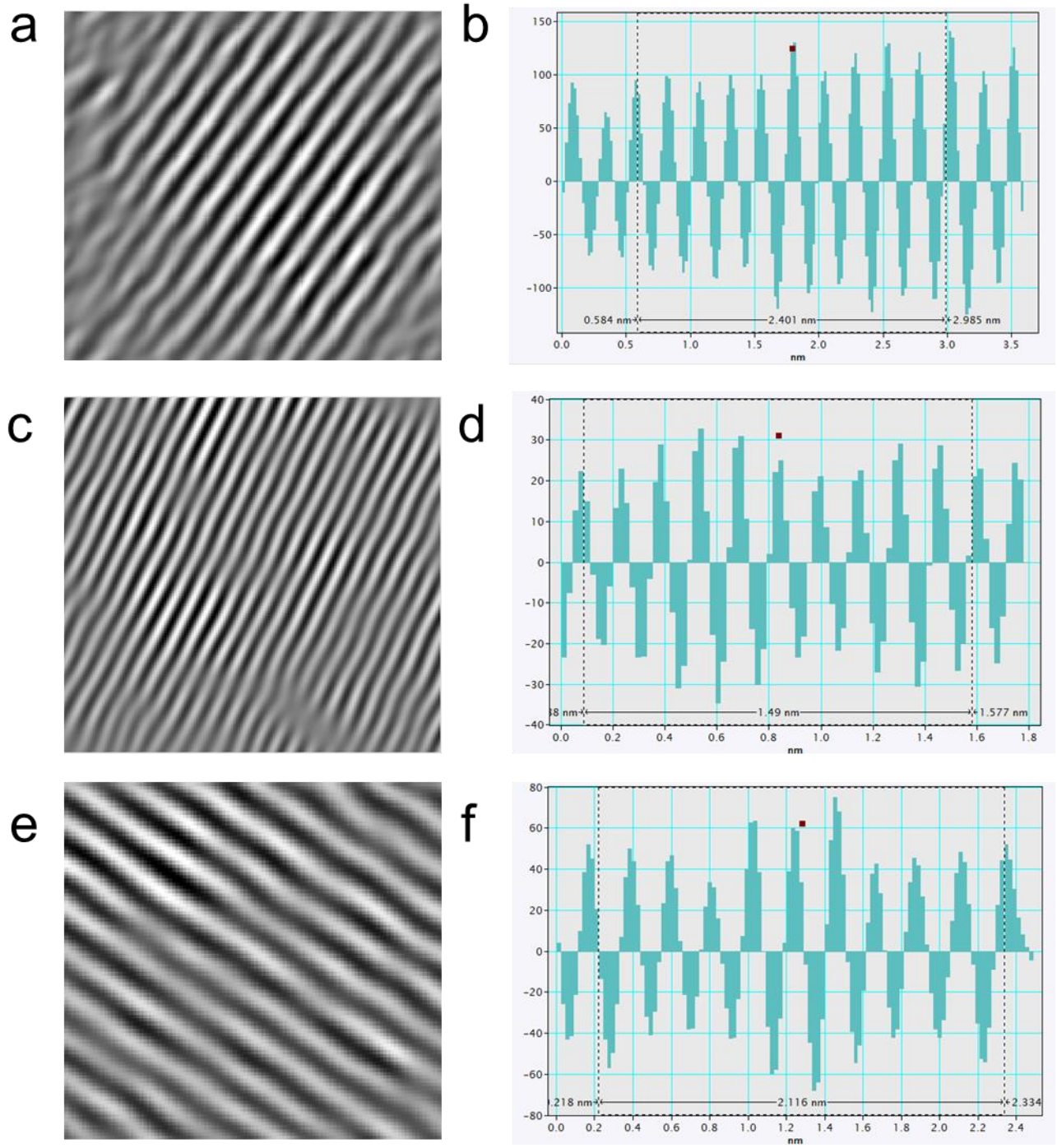

Supplementary Fig. 9 a,c,e Fourier-filtered image and **b,d,f** corresponding line intensity profiles for (111), (220) and (200) crystal planes of Nano-NiO.

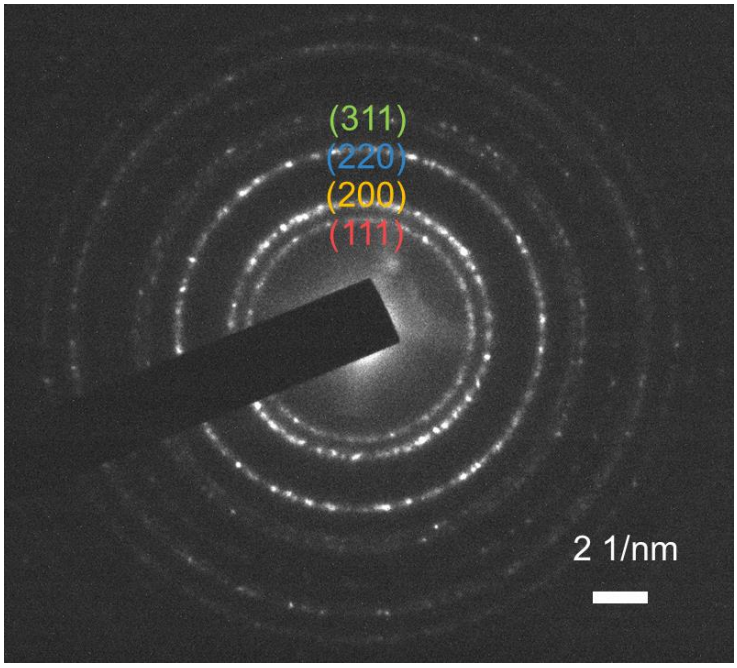

Supplementary Fig. 10 SAED image of Nano-NiO

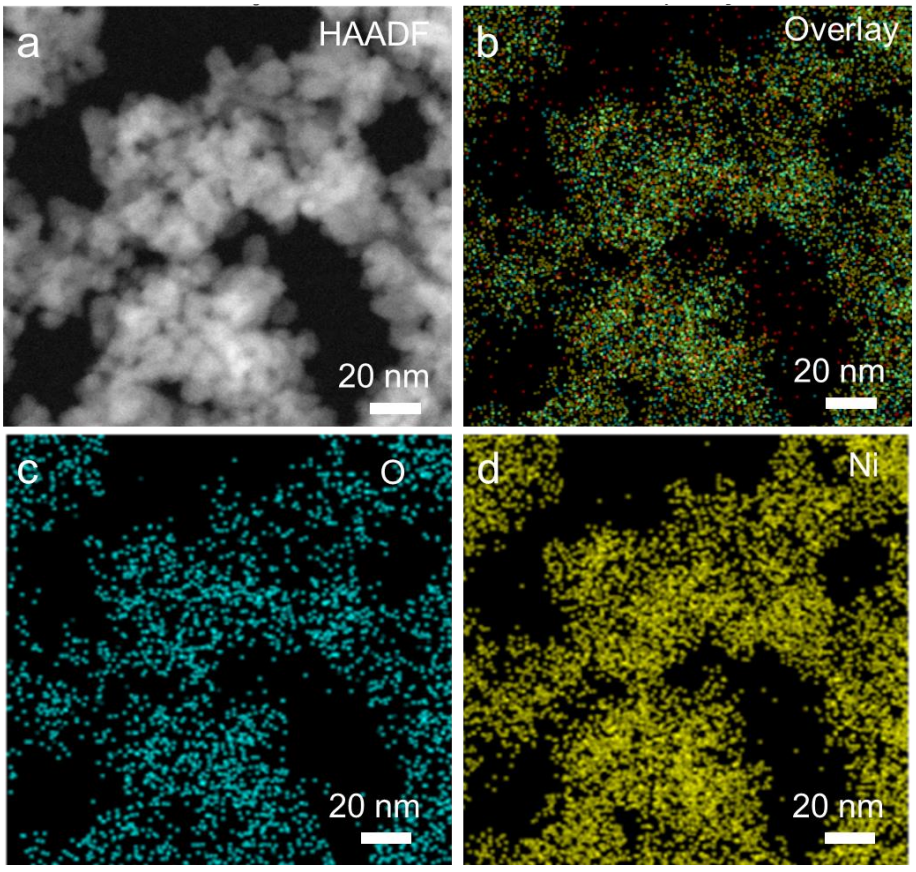

Supplementary Fig. 11 a HAADF-STEM image and the corresponding EDS elemental mapping images for the **b** overlay, **c** O (indigo), and **d** Ni (yellow) distributions on Nano-NiO.

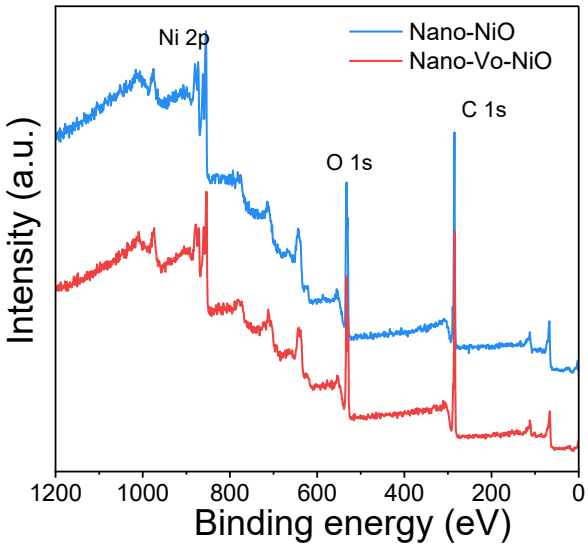

Supplementary Fig. 12 Survey scan XPS spectra of Nano-NiO and Nano-Vo-NiO.

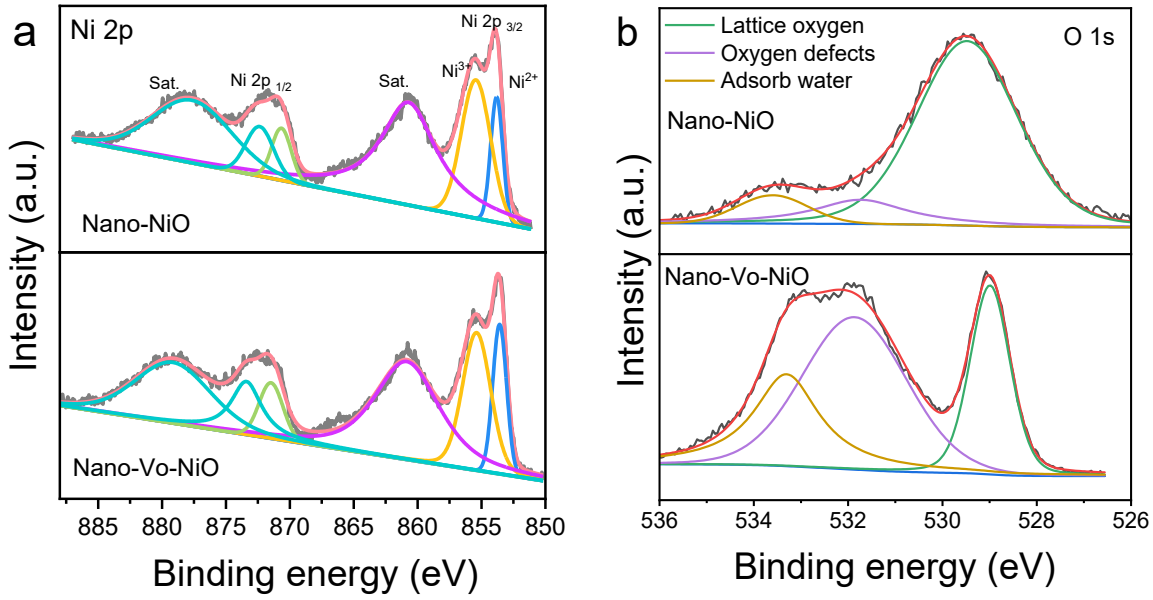

Supplementary Fig. 13 High-resolution XPS spectra of **a** Ni 2p, **b** O 1s of Nano-NiO and Nano-Vo-NiO.

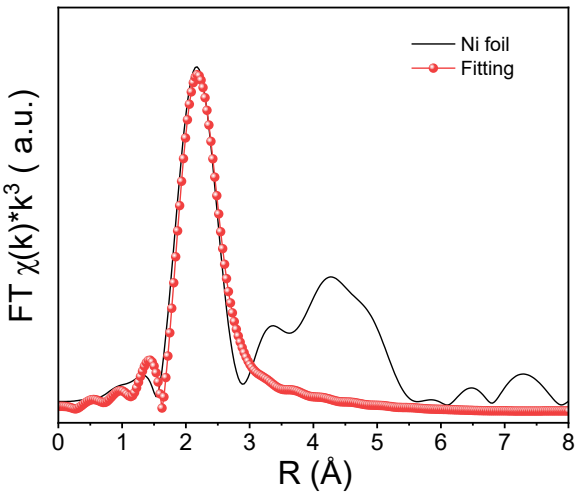

Supplementary Fig. 14 FT-EXAFS curves for the experimental data and the fitted profiles at the Ni K-edge of Ni foil.

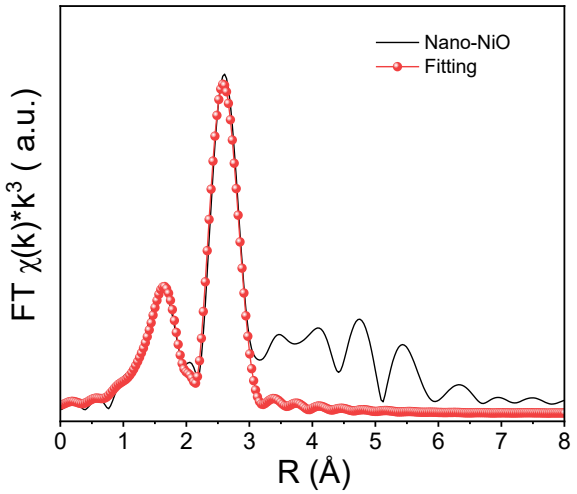

Supplementary Fig. 15 FT-EXAFS curves for the experimental data and the fitted profiles at the Ni K-edge of Nano-NiO.

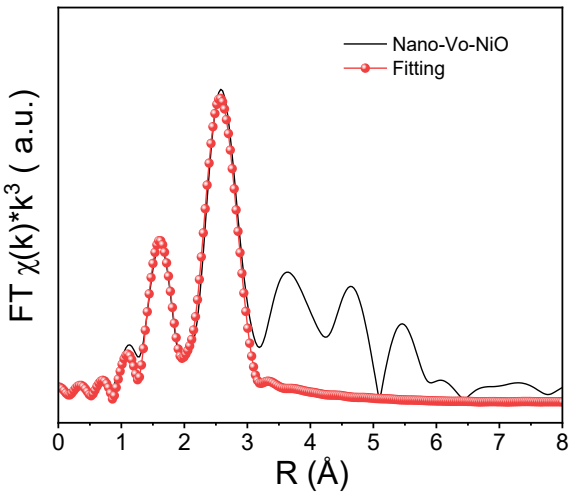

Supplementary Fig. 16 FT-EXAFS curves for the experimental data and the fitted profiles at the Ni K-edge of Nano-Vo-NiO.

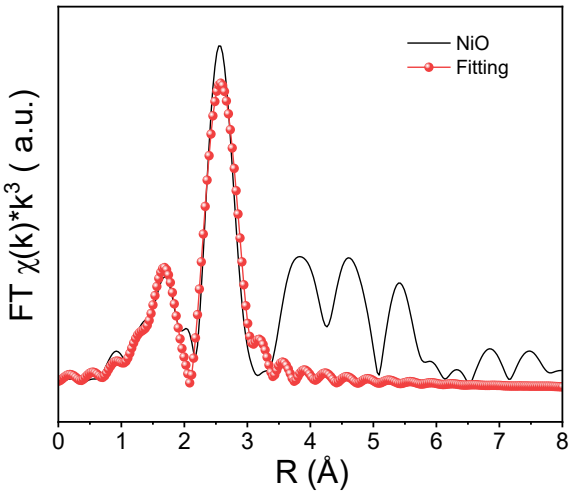

Supplementary Fig. 17 FT-EXAFS curves for the experimental data and the fitted profiles at the Ni K-edge of NiO.

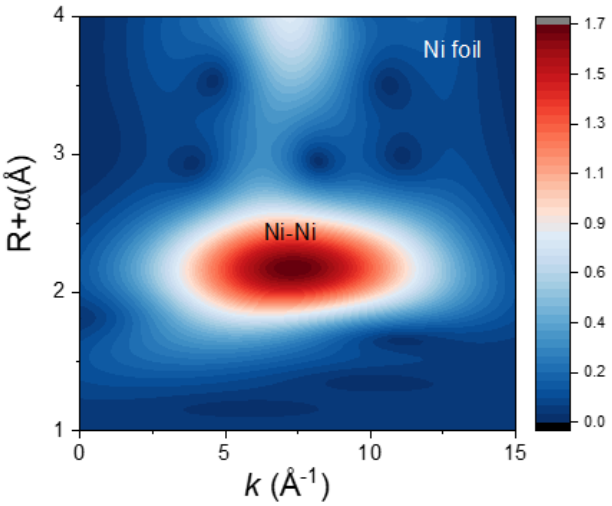

Supplementary Fig. 18 Wavelet transform of Ni K-edge on Ni foil.

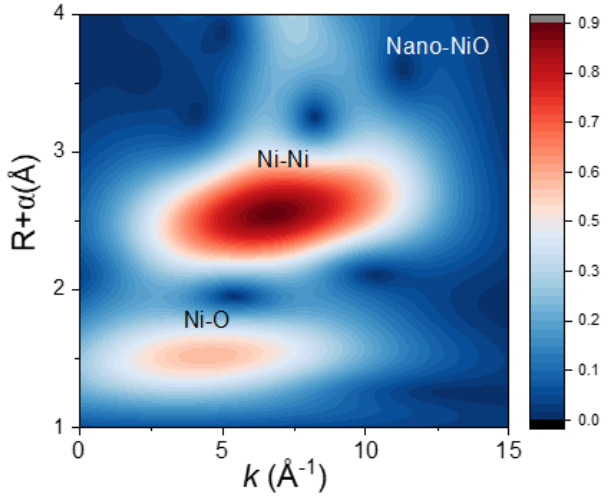

Supplementary Fig. 19 Wavelet transform of Ni K-edge on Nano-NiO.

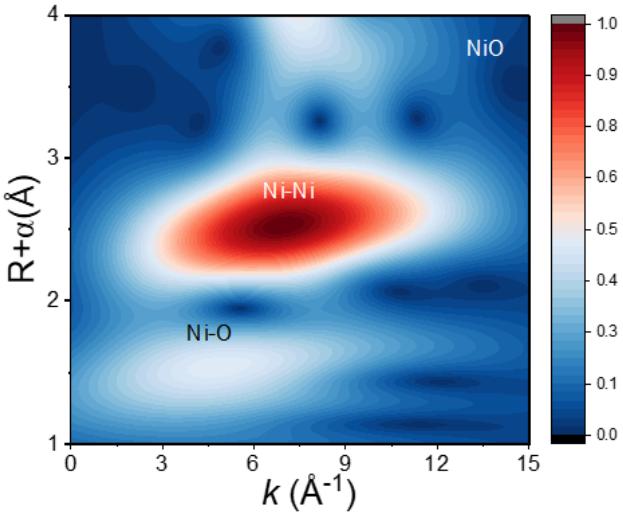

Supplementary Fig. 20 Wavelet transform of Ni K-edge on NiO.

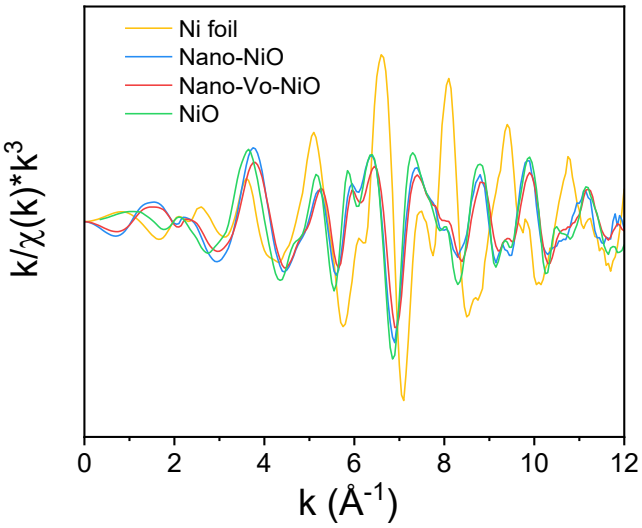

Supplementary Fig. 21 k^3-weighted raw EXAFS spectra at the Ni K-edge of Nano-NiO, Nano-Vo-NiO, Ni foil, and NiO.

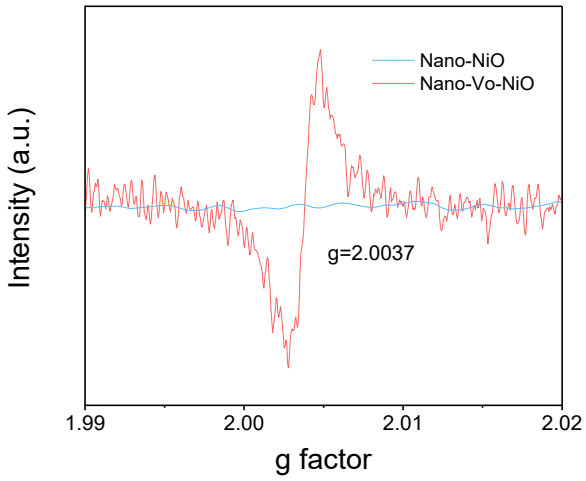

Supplementary Fig. 22 EPR spectra of Nano-NiO and Nano-Vo-NiO.

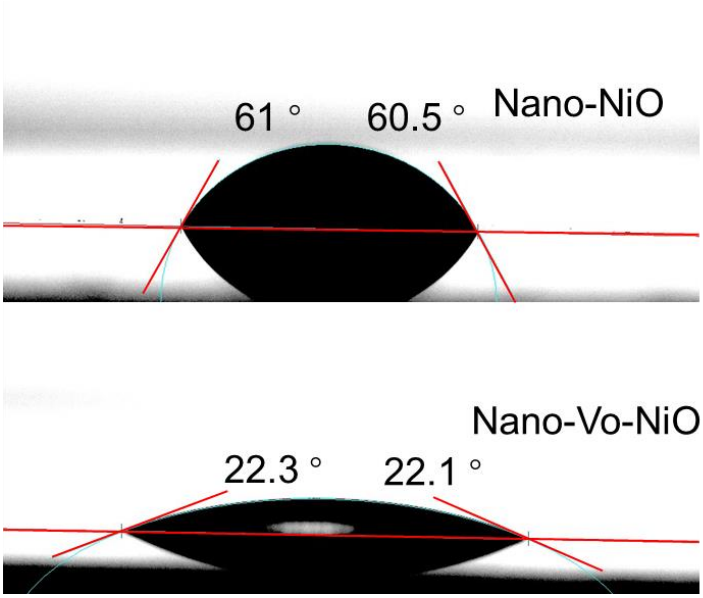

Supplementary Fig. 23 Optical contact angle measurements of Nano-NiO and Nano-Vo-NiO.

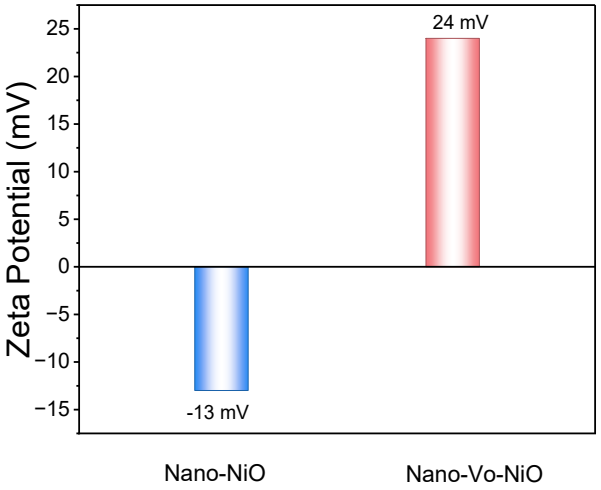

Supplementary Fig. 24 Zeta potential of Nano-NiO and Nano-Vo-NiO.

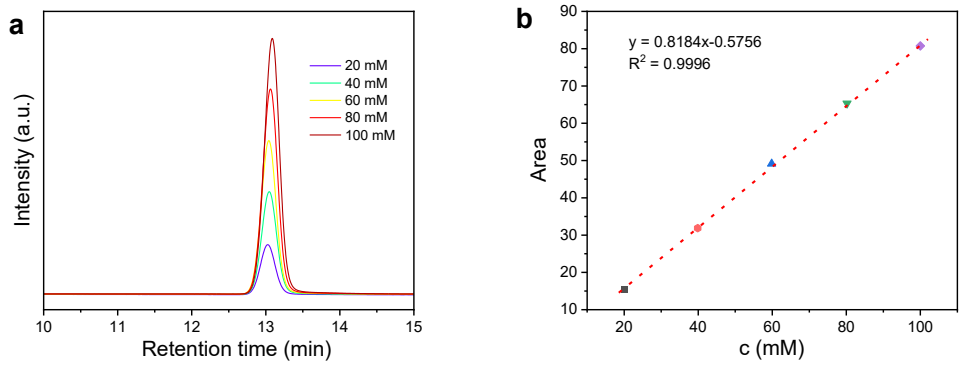

Supplementary Fig. 25 a Standard curves and **b** HPLC chromatograms of HCOOH.

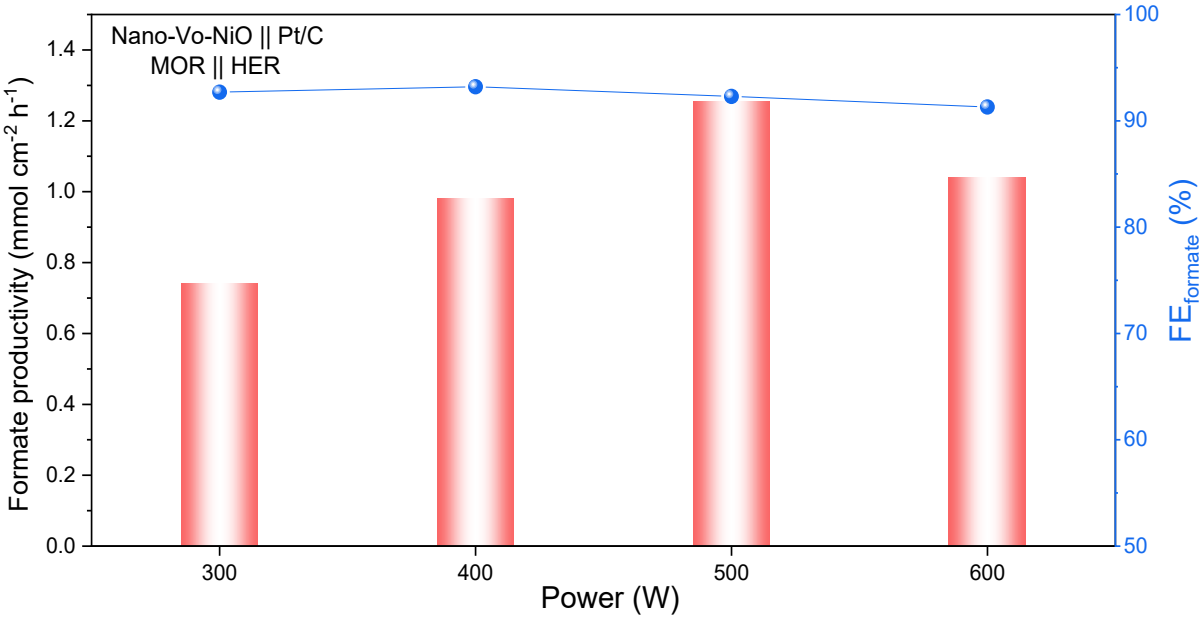

Supplementary Fig. 26 The performance of electrocatalysts in catalyzing methanol oxidation corresponds to different plasma treatment powers.

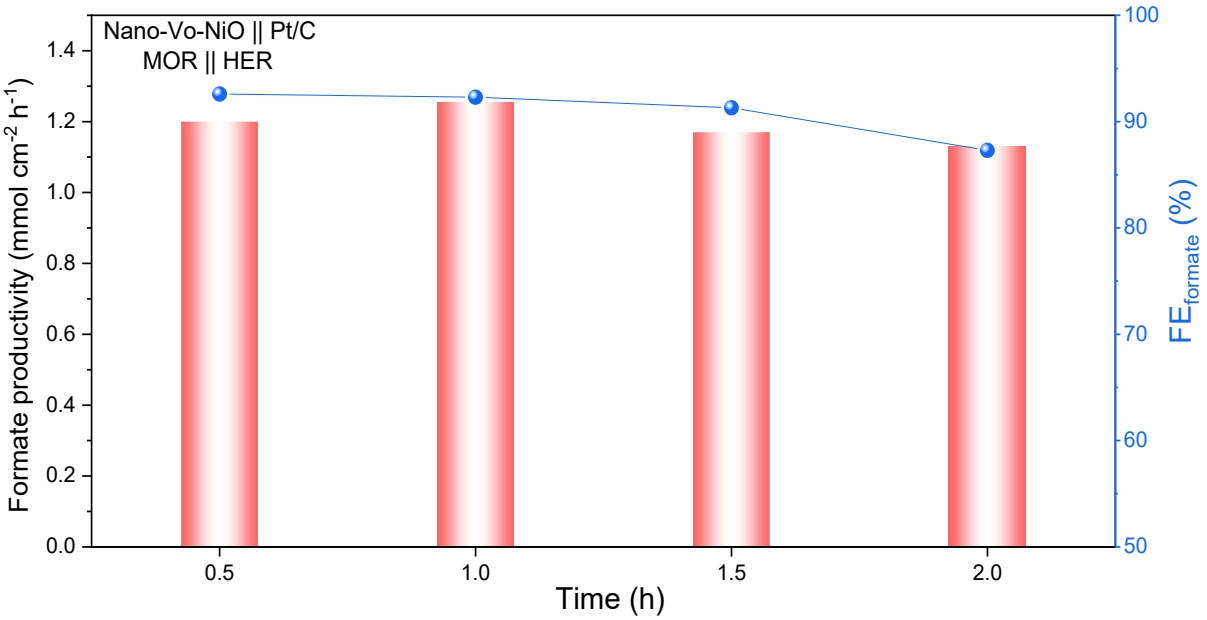

Supplementary Fig. 27 The performance of electrocatalysts in catalyzing methanol oxidation corresponds to different plasma treatment time.

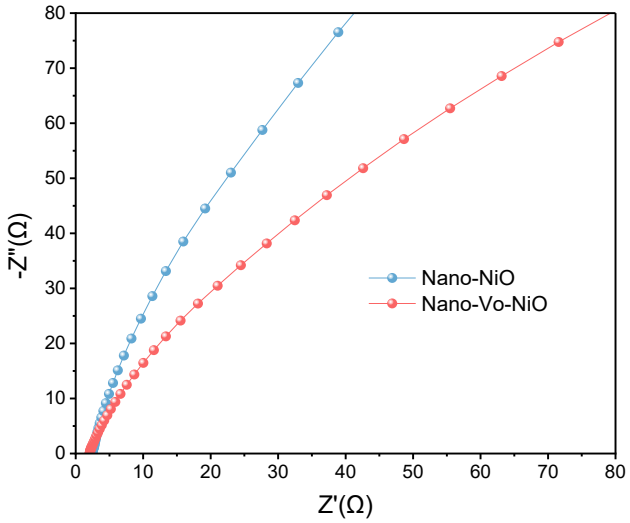

Supplementary Fig. 28 EIS Nyquist curves of Nano-NiO and Nano-Vo-NiO in 1.0 M KOH at the open-circuit potential.

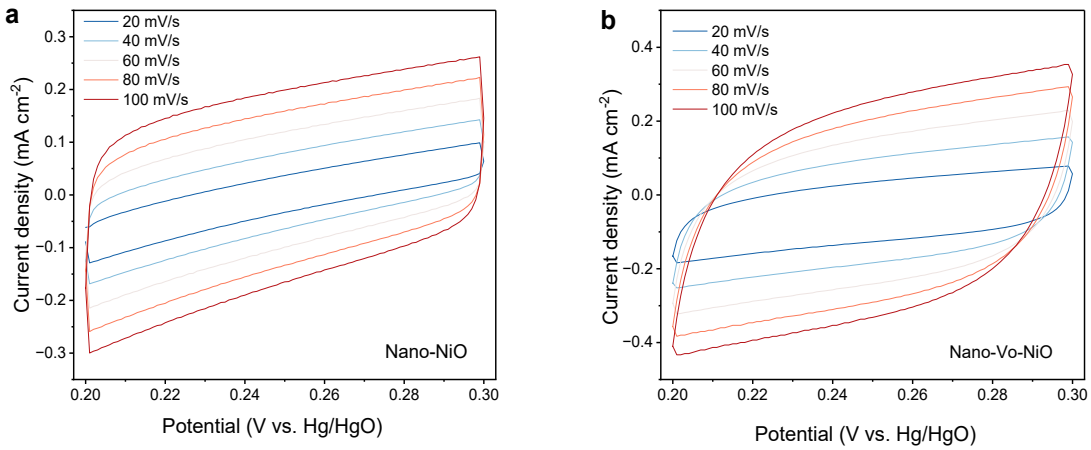

Supplementary Fig. 29 CV curves of **a** Nano-NiO and **b** Nano-Vo-NiO over non-Faradic potential range at scan rates of 20, 40, 60, 80, and 100 mV s^{-1}.

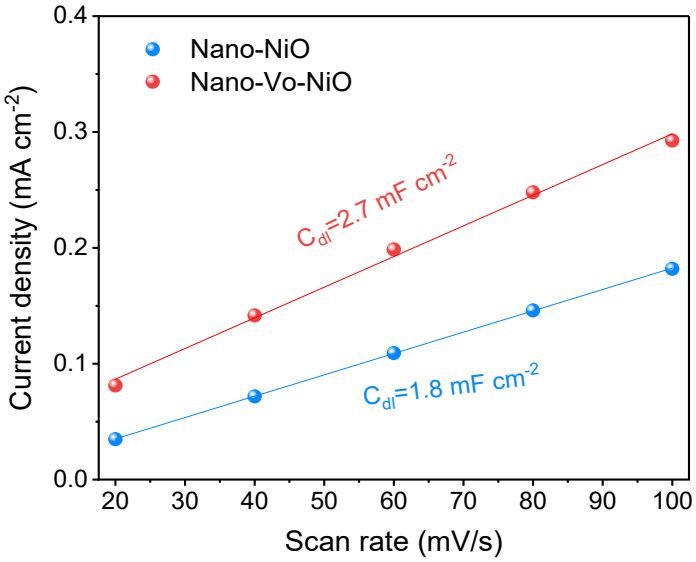

Supplementary Fig. 30 Electrochemical double-layer capacitances (C_{dl}) values of Nano-NiO and Nano-Vo-NiO.

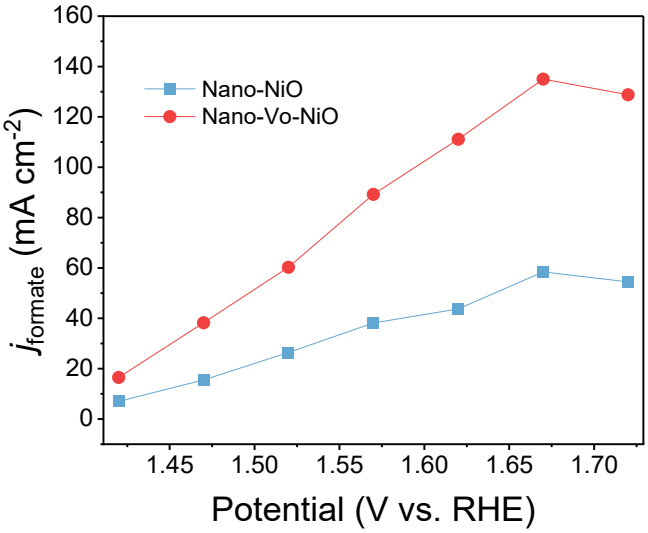

Supplementary Fig. 31. $j_{formate}$ at varied voltages of Nano-NiO and Nano-Vo-NiO in an H-type cell.

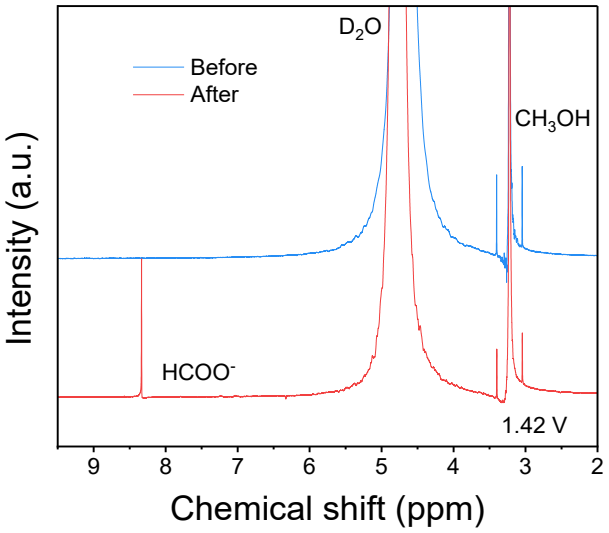

Supplementary Fig. 32 ^{1}H NMR spectra of electrolytes before and after electrolysis.

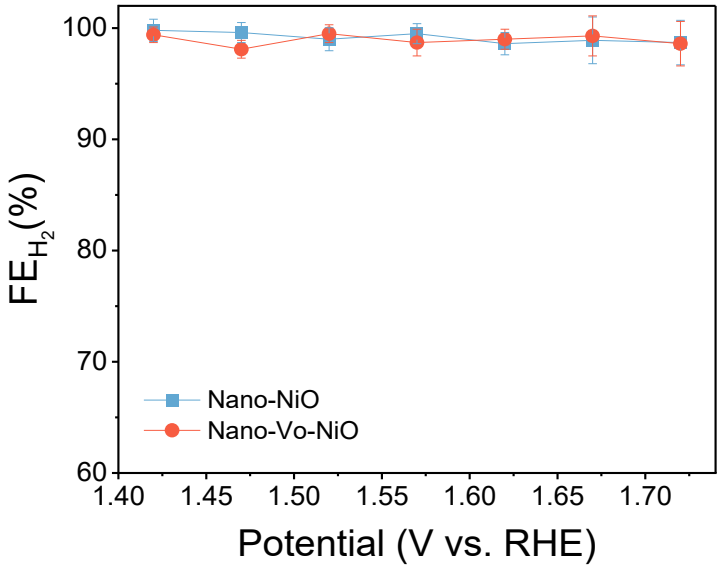

Supplementary Fig. 33 The Faradaic efficiency of hydrogen at varied potential MOR coupled HER system in an H-type cell.

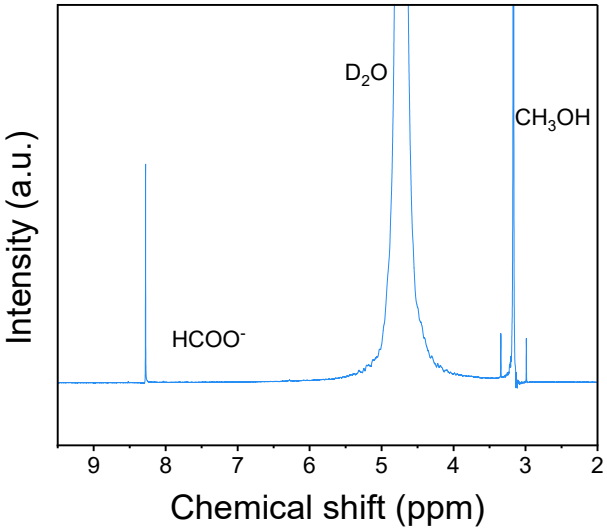

Supplementary Fig. 34 ^{1}H NMR spectra of electrolytes after electrolysis in a long-term stability test at the potential of 1.6 V vs. RHE.

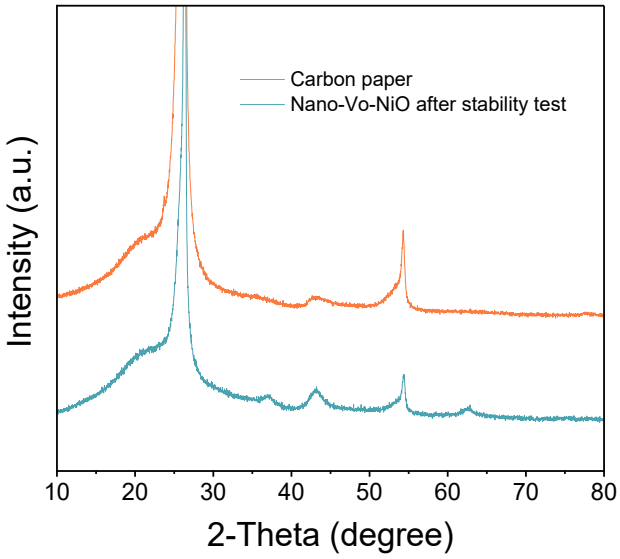

Supplementary Fig. 35 XRD pattern of Nano-Vo-NiO after stability test.

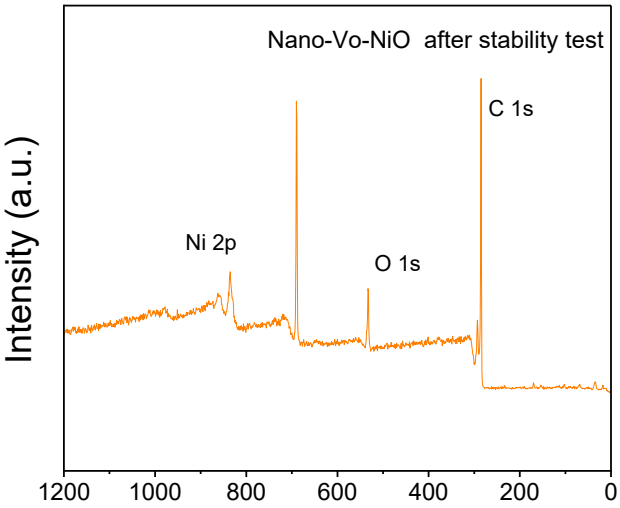

Supplementary Fig. 36 Survey scan XPS spectra of f Nano-Vo-NiO after stability test.

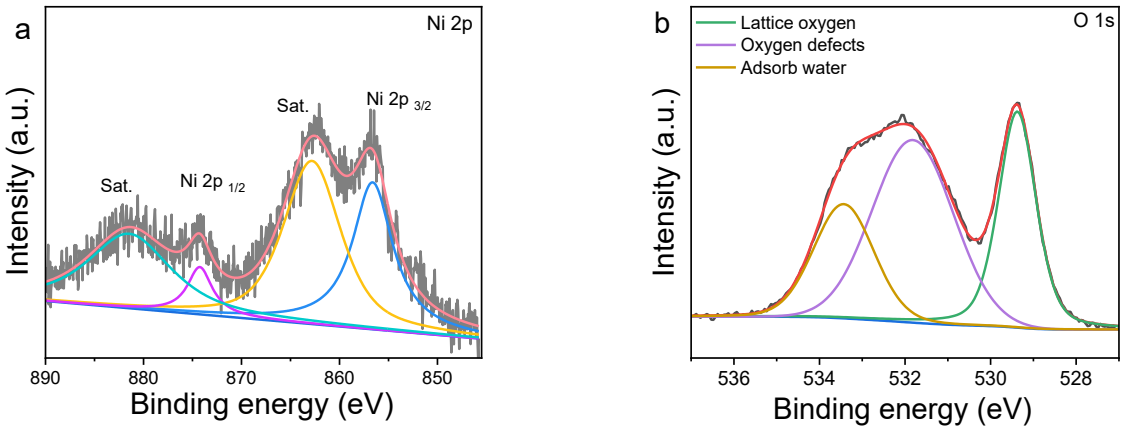

Supplementary Fig. 37 High-resolution XPS spectra of **a** Ni 2p, **b** O 1s of Nano-Vo-NiO after stability test.

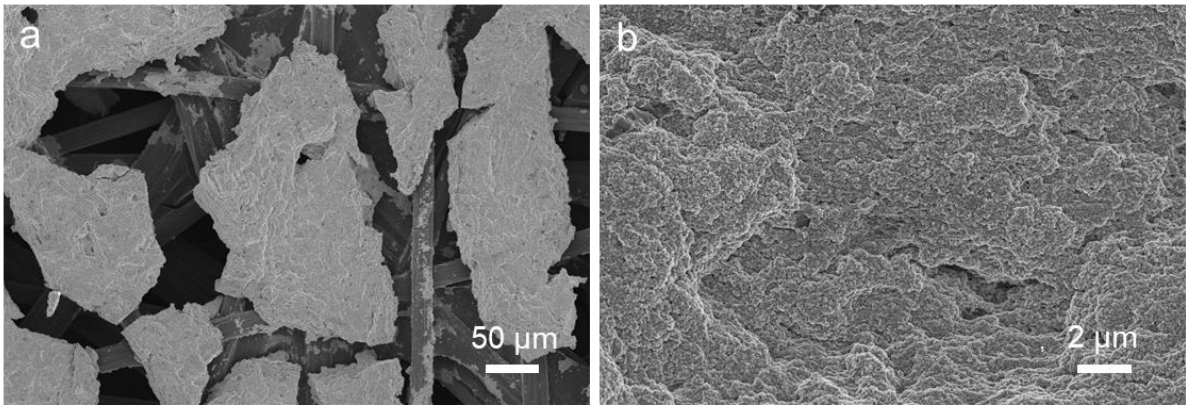

Supplementary Fig. 38 SEM images of Nano-Vo-NiO after stability test.

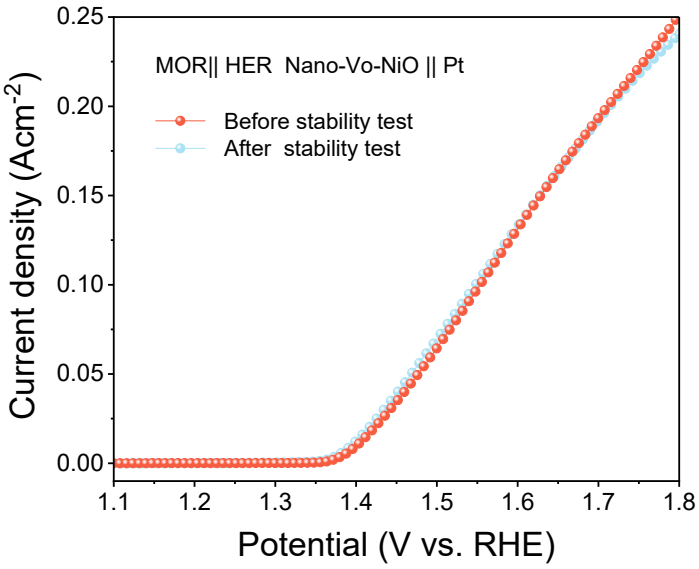

Supplementary Fig. 39 LSV curves in 1 M KOH with or without 1 M CH_3OH of Nano-Vo-NiO before and after stability test.

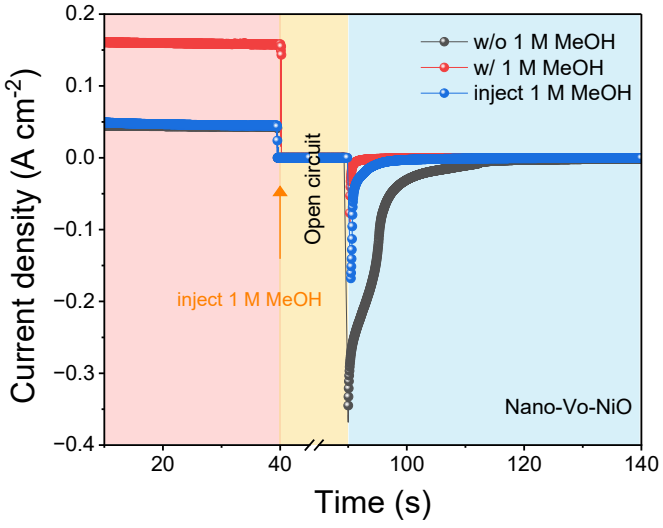

Supplementary Fig. 40 Multipotential step curves of Nano-Vo-NiO in 1 M KOH solutions without and with 1 M MeOH. In all panels, the pink, orange, and pale shaded areas indicate the application of a constant voltage of 1.60 V (vs. RHE), an open-circuit process, and the application of an open-circuit voltage of 1.1 V (vs. RHE), respectively.

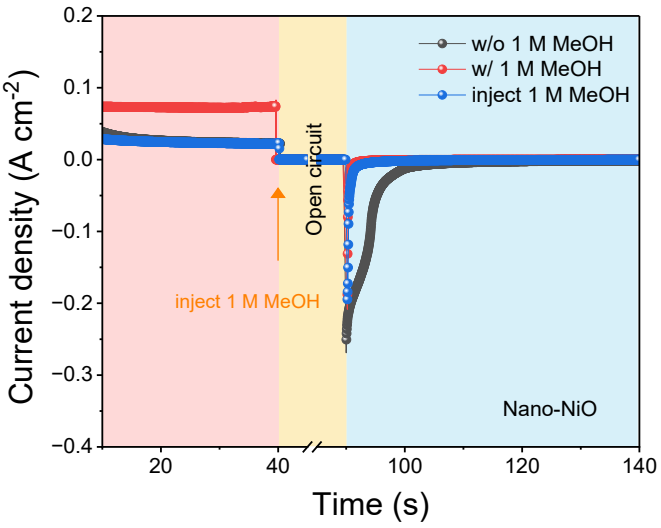

Supplementary Fig. 41 Multipotential step curves of Nano-NiO in 1 M KOH solutions without and with 1 M MeOH. In all panels, the pink, orange, and pale shaded areas indicate the application of a constant voltage of 1.60 V (vs. RHE), an open-circuit process, and the application of an open-circuit voltage of 1.1 V (vs. RHE), respectively.

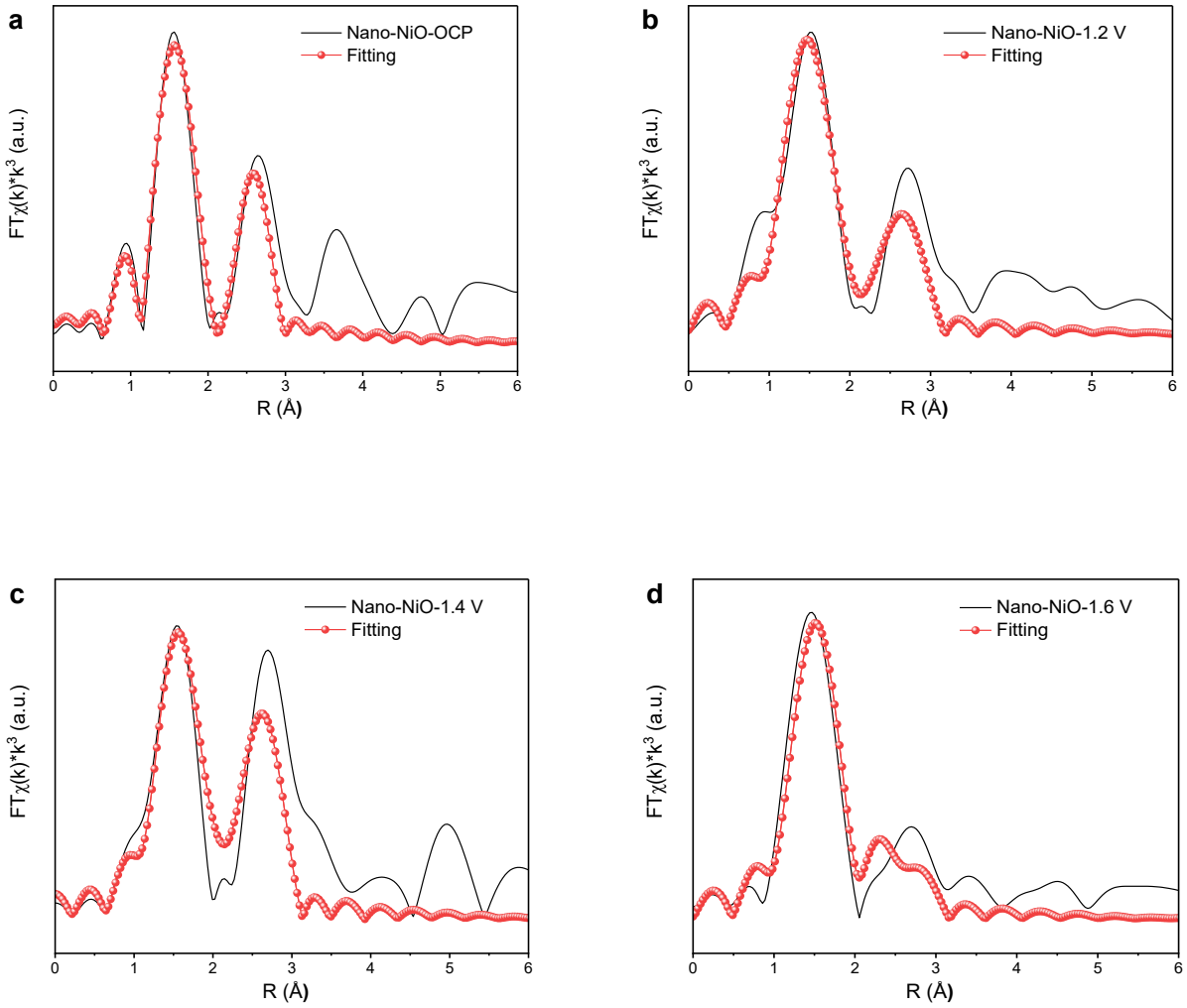

Supplementary Fig. 42 Ni K-edge FT-EXAFS curves for the experimental and fitted profiles of Nano-NiO in 1 M KOH at **a** OCP, **b** 1.2 V, **c** 1.4 V, **d** 1.6 V (vs. RHE).

.

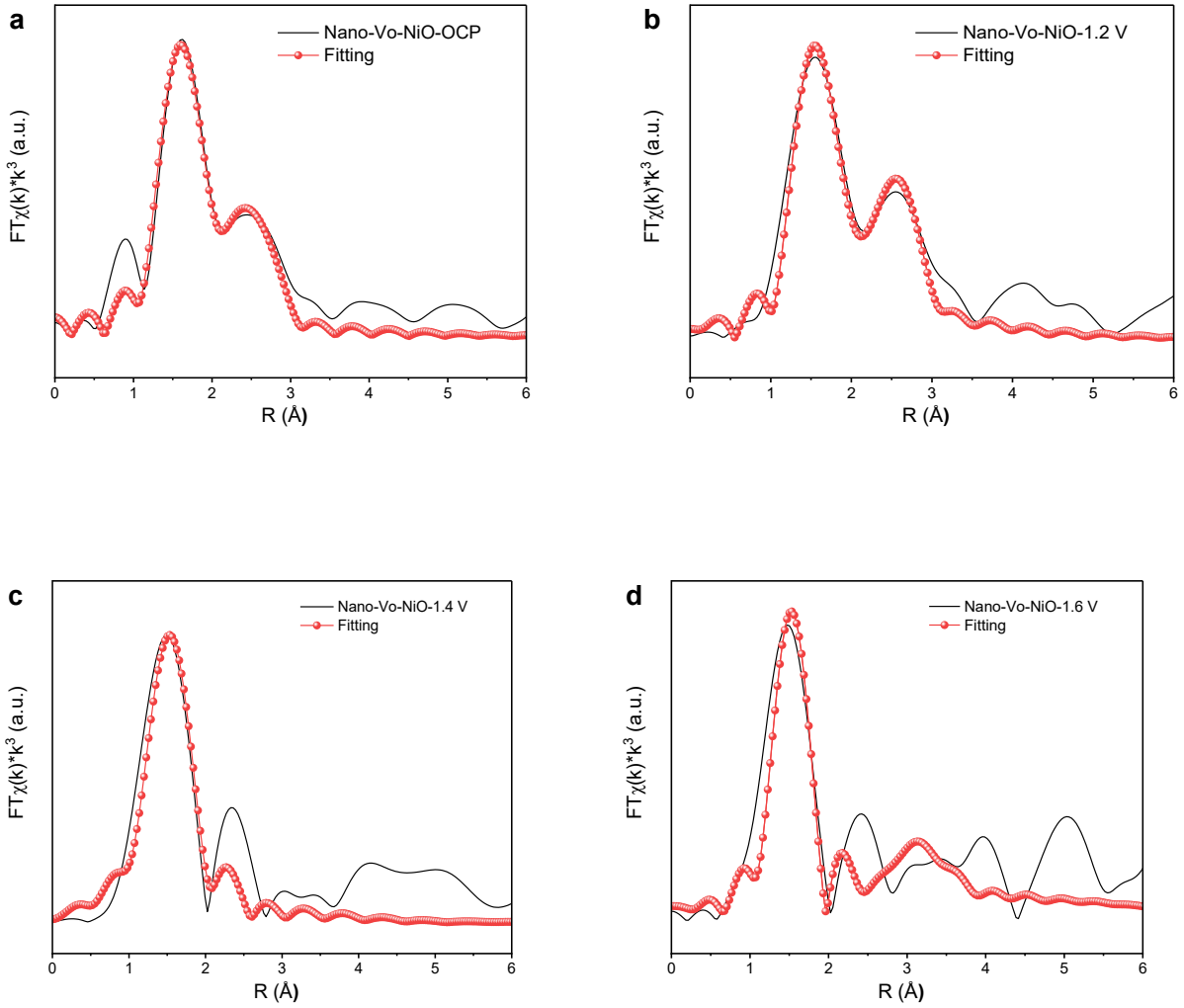

Supplementary Fig. 43 Ni K-edge FT-EXAFS curves for the experimental and fitted profiles of Nano-Vo-NiO in 1 M KOH at **a** OCP, **b** 1.2 V, **c** 1.4 V, **d** 1.6 V (vs. RHE).

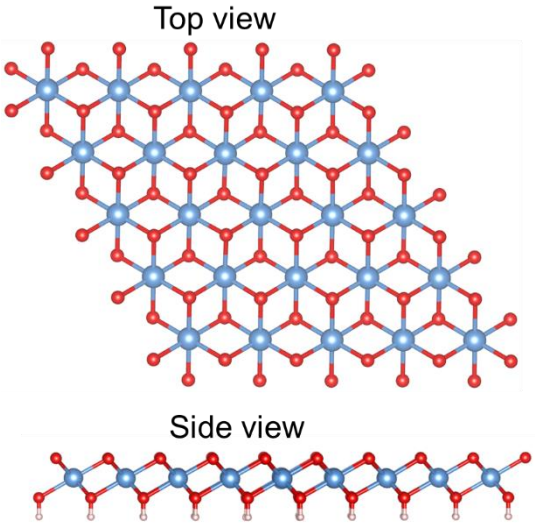

Supplementary Fig. 44 Top- and side-view models of Nano-NiO.

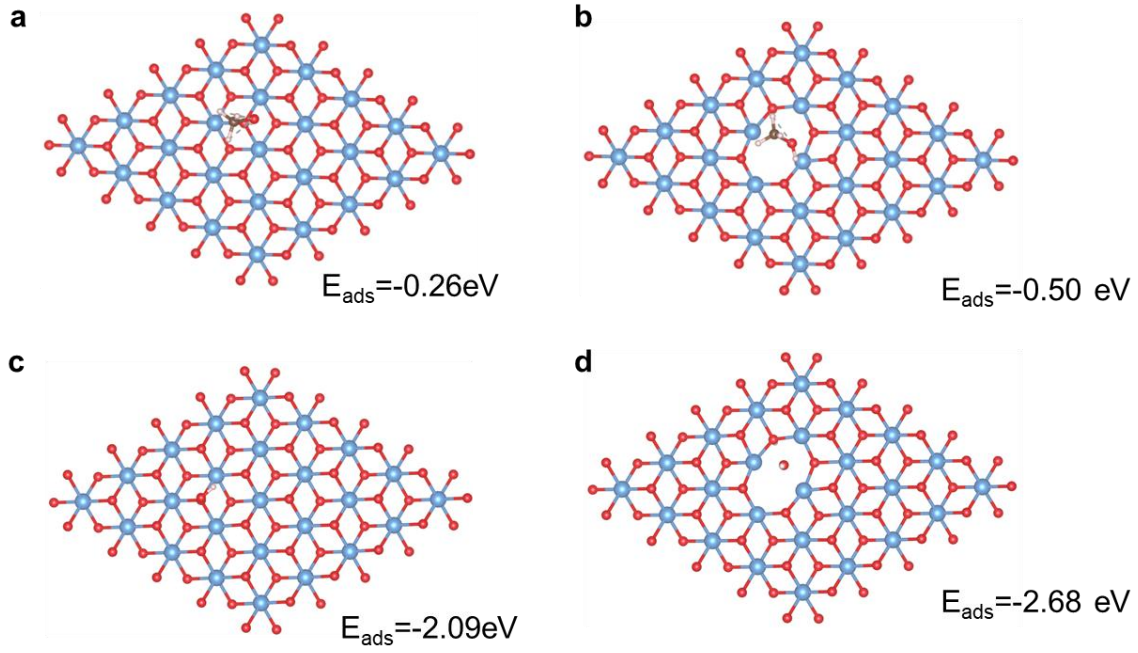

Supplementary Fig. 45 Adsorption energy and configurations of **a, b** CH_3OH*and **c,d** OH* on Nano-NiO and Nano-Vo-NiO. The blue, light pink, brown and red balls represent the Ni, H, C and O atoms, respectively.

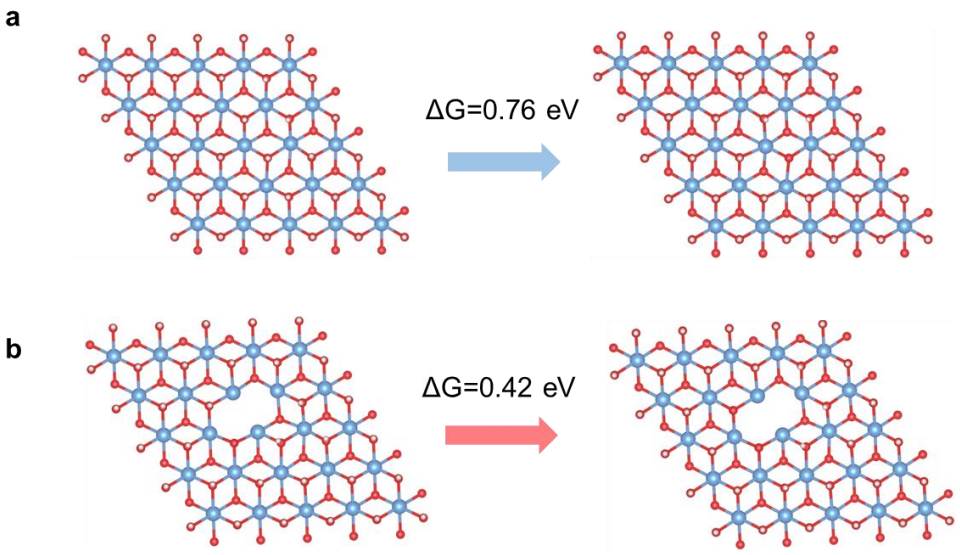

Supplementary Fig. 46 Free energy and configuration profiles for deintercalation of the proton of **a** Nano-NiO and **b** Nano-Vo-NiO. The blue, light pink, brown and red balls represent the Ni, H, C and O atoms, respectively.

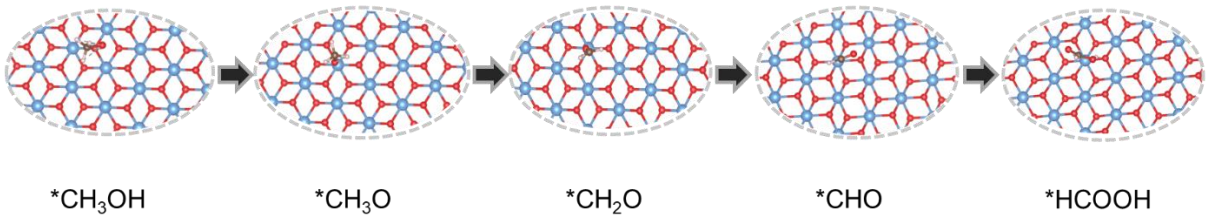

Supplementary Fig. 47 The intermediate configurations during electrocatalytic methanol oxidation on Nano-NiO. The blue, light pink, brown and red balls represent the Ni, H, C and O atoms, respectively.

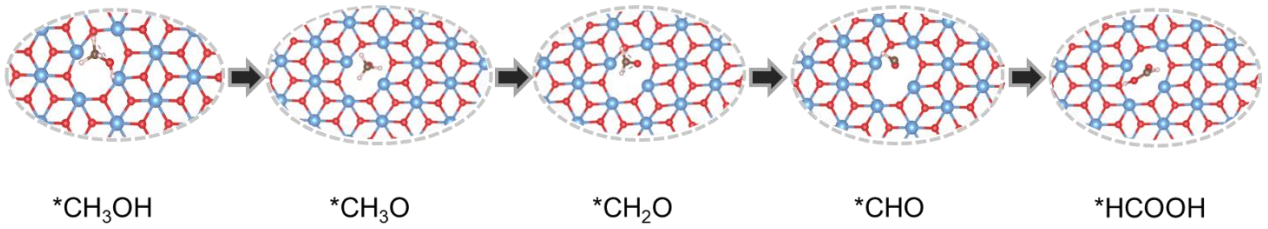

Supplementary Fig. 48 The intermediate configurations during electrocatalytic methanol oxidation on Nano-Vo-NiO. The blue, light pink, brown and red balls represent the Ni, H, C and O atoms, respectively.

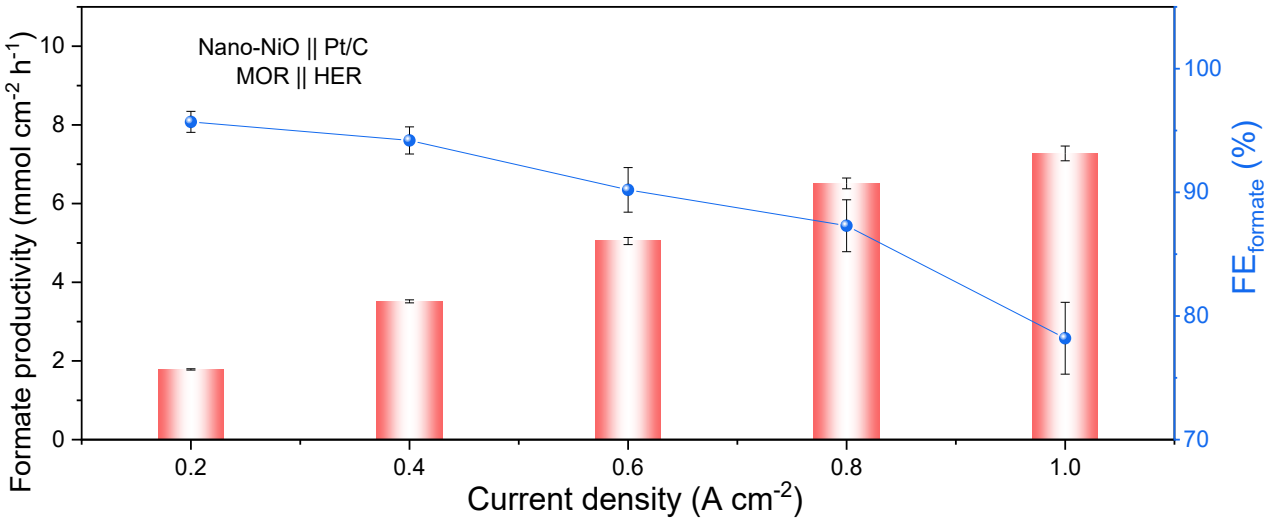

Supplementary Fig. 49 Formate production rate and $FE_{formate}$ at varied current density of Nano-NiO for MOR || HER electrolysis systems in MEA electrolyzer.

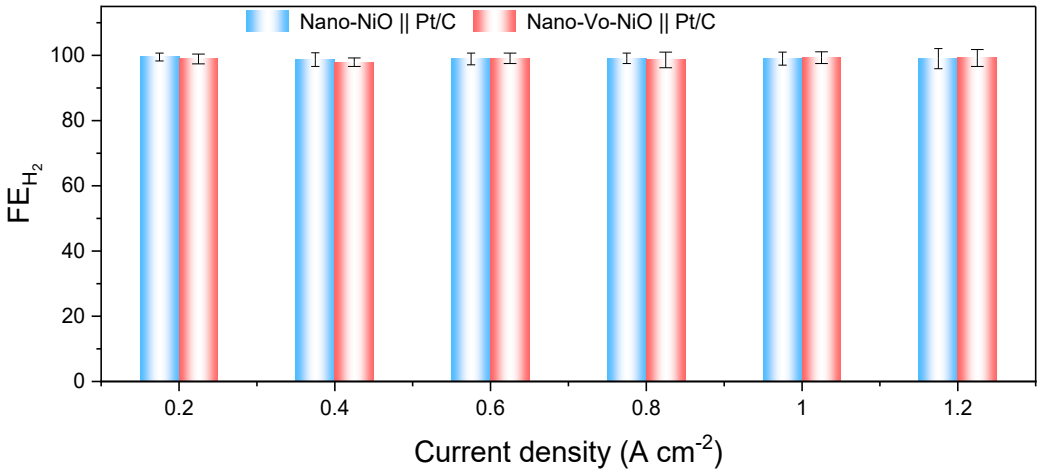

Supplementary Fig. 50 The Faraday efficiency of hydrogen at varied current density for || HER electrolysis systems in MEA electrolyzer.

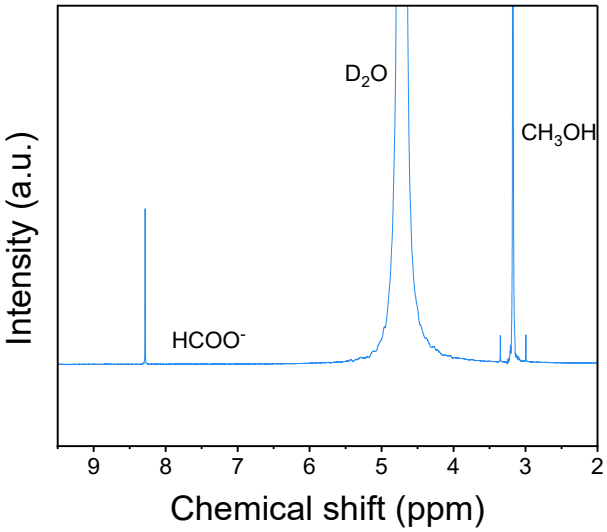

Supplementary Fig. 51 ^{1}H NMR spectra of electrolytes after electrolysis in a two-electrode MEA electrolyzer.

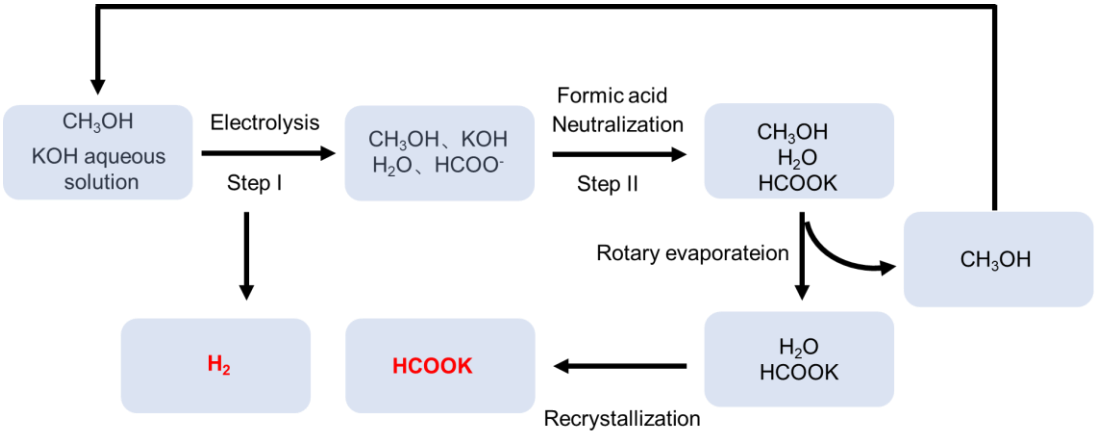

Supplementary Fig. 52 Schematic diagram of the operation unit for the integrated process of electrocatalytic oxidation of methanol and hydrogen production.

Supplementary Note. 1

Techno-economic Analysis

To evaluate the economic feasibility of electrocatalytic methanol oxidation coupled with hydrogen evolution for value-added upgrading, a simplified techno-economic analysis model was employed. We adopted a simplified techno-economic analysis model, which draws on the methods reported in published literature[1-5]. It is assumed that the plant has an annual processing capacity of 10,000 tons of methanol. Key economic parameters and assumptions are detailed in Supplementary Table 7. The detailed techno-economic analysis is as follows:

1. Capital costs

1.1 Total installed cost [6]

1.1.1 Production process cost

In the electrocatalytic methanol oxidation process, based on economic assumptions, the cost of the electrolytic cell can be obtained by the following formula.

$$\text{Area of electrolyzer} = \frac{\text{annual glycerol processing capacity}}{\text{conversion rate at operating current density} \times \text{operating time}}$$

$$\text{Electrolyzer Cost} = 10{,}000 \text{ US dollars per square meter} \times \text{Electrolyzer Area}$$

Annual methanol processing capacity: 10,000 tons; Conversion rate at operating current density (300 mA/cm²): 0.0851 g/(cm²·h).

Therefore, Electrolyzer Area = 10,000,000,000 / (0.0851 × 24 × 300 × 10,000) = 10,000,000,000 / 612,720,000 = 1632.07 m², and electrolyzer cost = 16,320,668.4 US dollars.

The cost of electrocatalysts and membranes accounts for 5% of the electrolyzer cost, which is 816,033.4 US dollars. The cost of other equipment (including pumps, computers, software, etc.) is assumed to be 10% of the electrolyzer cost, with a total cost of 1,632,066.8 US dollars.

The production process cost of the electrocatalytic process can be calculated by the following formula:

Production Process Cost = Electrolyzer Cost + Cost of Electrocatalysts and Membranes + Cost of Other Equipment

The production process cost of the electrocatalytic process is 16,320,668.4 + 816,033.4 + 1,632,066.8 = 18,768,768.6 US dollars.

1.1.2 Product separation cost

Assume that the product separation cost accounts for 50% of the production process cost. (ACS Sustainable Chem. Eng. 5, 6626-6634 (2017)

Product separation cost = 50% × Production process cost

For the electrocatalytic methanol oxidation process, product separation cost = 50% × 18,768,768.6 = 9,384,384.3 US dollars.

1.1.3 Waste treatment device cost

The waste treatment system is designed to handle solid waste and wastewater generated during the production process. The cost of the waste treatment system is estimated to account for 8% of the total Production process cost and Product separation costs.

Waste treatment device cost = (18,768,768.6 + 9,384,384.3) × 8% = 2,252,252.2 US dollars.

1.1.4 Additional utility cost

Additional utility costs include expenses for other parts of the plant and can be assumed to account for 5% of the total installed cost.

1.1.5 Total Installation Cost

Total Installation Cost = Production process cost + Product separation cost + Waste Treatment device cost + Additional utility cost

For the electrocatalytic methanol oxidation process, Total Installed Cost = $(18,768,768.6 + 9,384,384.3 + 2,252,252.2) / 0.95 = 32,005,689.5 US dollars.

1.2 Total direct costs

1.2.1 Warehouse cost

The Warehouse Cost can be assumed to account for 4% of the Inside Battery Limits (IBL) Equipment Cost. The Inside Battery Limits (IBL) Equipment Cost includes the Production process cost and Product separation cost.

Warehouse cost = 4% × (Production process cost + Product separation cost) = 0.04 × (18,768,768.6 + 9,384,384.3) = 1,126,126.1 US dollars.

1.2.2 Site development cost

The Site development cost can be assumed to account for 9% of the Inside Battery Limits (IBL) Equipment Cost. The Inside Battery Limits (IBL) Equipment Cost includes the Production process cost and Product separation cost.

Site development cost = 9% × (Production process cost + Product separation cost)

For the electrocatalytic methanol oxidation process, Site development cost = 0.09 × (18,768,768.6 + 9,384,384.3) = 2,533,783.7 US dollars.

1.2.3 Additional piping cost

The Additional piping cost can be assumed to account for 4.5% of the Inside Battery Limits (IBL) Equipment Cost. The Inside Battery Limits (IBL) Equipment Cost includes the Production process cost and Product separation cost.

Additional Piping Cost = 4.5% × (Production process cost + Product separation cost)

For the electrocatalytic methanol oxidation process, Additional piping cost = 0.045 × (18,768,768.6 + 9,384,384.3) = 1,266,891.9 US dollars.

1.2.4 Total direct cost

Total direct cost = Total installed cost + Warehouse cost + Site development cost + Additional piping cost.

For the electrocatalytic methanol oxidation process, the Total direct cost = 32,005,689.5 + 1,126,126.1 + 2,533,783.7 + 1,266,891.9 = 36,932,491.2 US dollars.

1.3 Total Indirect Cost

1.3.1 Maintenance Cost

Maintenance Cost can be assumed to account for 10% of the Total direct cost, including the refurbishment costs of electrocatalysts and membranes.

1.3.2 Field cost

Field Cost can be assumed to account for 10% of the Total direct cost.

1.3.3 Building and construction cost

Building and Construction Costs can be assumed to account for 20% of the Total direct cost.

1.3.4 Other cost

Other Costs include licenses, sales and marketing expenses, research and development (R&D) expenses, financial expenses, etc. Other costs can be assumed to account for 10% of the Total direct cost.

1.3.5 Total indirect costs

Total indirect costs = Maintenance cost + Field cost + Building and construction cost + Other cost.

Total Indirect Costs = 36,932,491.2 × (0.1 + 0.1 + 0.2 + 0.1) = 18,466,245.6 US dollars.

1.4 Fixed capital investment

Fixed capital investment = Total direct costs + Total indirect costs

For the electrocatalytic methanol oxidation process, Fixed capital investment = 36,932,491.2 + 18,466,245.6 = 55,398,736.8 US dollars.

1.5 Total capital investment

Land cost is assumed to account for 1% of the Fixed capital investment.

Working capital cost is assumed to account for 5% of the Fixed capital investment.

Total Capital Investment = Fixed capital investment + Land cost + Working capital cost

For the electrocatalytic methanol oxidation process, Total capital investment = 55,398,736.8 × (1 + 0.01 + 0.05) = 58,722,661.0 US dollars.

The salvage value of the equipment after 15 years of operation is: 58,722,661 × (1 - 0.06)^15 = 23,213,037.9 US dollars.

1.6 Annual total capital investment

Annual total capital investment = (Total capital investment - Equipment Salvage Value) / Equipment Service Life

For the electrocatalytic methanol oxidation process, the annual total capital investment = (58,722,661-23,213,037.9)/15 = 2,367,308.2 US dollars.

2. Annual operating cost[1,2]

2.1 Annual raw material cost

Raw material costs account for the largest proportion of operating costs.

For the electrocatalytic methanol oxidation process, the raw materials include methanol, water, and potassium hydroxide, while the main products are potassium formate and hydrogen.

The specific balanced chemical equation is as follows:

$$CH_3OH + KOH + H_2O \rightarrow HCOOK + 3H_2\uparrow$$

Annual raw material consumption (assumed under conventional industrial operating conditions): 10,000 tons of methanol, 17,500 tons of potassium hydroxide, and 5,625 tons of water; the products include 1,875 tons of hydrogen and 26,250 tons of potassium formate (HCOOK).

Raw material cost = Methanol cost + Water cost + Potassium hydroxide cost = 10,000 × 340 +

17,500 × 820 + 5,625 × 0.22 = 17,751,237.5 US dollars

Annual Raw Material Costs = 17,751,237.5 US dollars

2.2 Annual utility operating cost

Utility operating costs account for the second-largest proportion of operating costs, including electricity, thermal energy, steam, cooling water, etc.

2.2.1 Annual electricity cost

For the electrocatalytic methanol process, the power (kW) required to sustain the plant's production can be calculated using the following formula, assuming an operating current density of 0.3 A/cm².

$$\text{Power (kW)} = (\text{Cell Voltage} \times \text{Operating Current Density} \times \text{Electrolyzer Area}) / 1000$$

$$\text{Annual Electricity Consumption (kWh)} = \text{Power (kW)} \times \text{Daily Operating Hours} \times 300 \text{ Days} \times \text{Electricity Price (US dollars per kWh)}$$

For the electrocatalytic methanol oxidation process, the power consumption is 8,704.2 kW, and the total primary electricity cost is 6,267,024 US dollars per year. Additionally, the electricity costs for lighting, machine electric drives, and other related expenses are assumed to be 626,702.4 US dollars. Therefore, the total electricity cost for the electrocatalytic process = 626,702.4 + 6,267,024 = 6,893,726.4 US dollars.

2.2.2 Annual costs for thermal energy, steam, and cooling water (Operating cost)

For the electrocatalytic methanol oxidation process, the costs for thermal energy, steam, and cooling water are assumed to account for 35% of the Raw material costs, covering the separation and waste treatment stages.

The corresponding costs are estimated to be 0.35 × 17,751,237.5 = 6,212,933.1 US dollars.

2.2.3 Annual utility operating cost

Annual Utility Operating Costs = Annual Electricity Costs + Costs for Thermal Energy, Steam, and Cooling Water

For the electrocatalytic methanol oxidation process, Annual Utility Operating Costs = 6,893,726.4 + 6,212,933.1 = 13,106,659.5 US dollars per year.

2.3 Other annual operating cost (Maintenance cost)

Waste treatment operating costs, transportation, storage, and fixed operating costs are included in the other operating costs.

The other operating costs are assumed to account for 5% of the raw material costs.

For the electrocatalytic process, Other Operating Costs = 17,751,237.5 × 0.05 = 887,561.9 US dollars per year.

2.4 Annual operating cost

Annual operating cost = Annual raw material cost + Annual utility operating cost + Other annual operating cost

For the electrocatalytic methanol oxidation process,

Annual operating cost = 17,751,237.5 + 13,106,659.5 + 887,561.9 = 31,745,458.9 US dollars.

3. Annual Revenue

For the electrocatalytic methanol oxidation process, considering the quality loss during the purification and separation process, the actual annual yield is 95% of the input raw materials.

The annual revenue of the electrocatalytic process can be calculated using the following formula:

Annual Revenue = Production mass of potassium formate (HCOOK) × Price of potassium formate + Production mass of hydrogen × Price of hydrogen

= 26265 × 0.95(FE) × 0.95(quality loss) × 1,590 + 1,875 × 0.95 × 1,900 = 37,668,054 + 3,384,375 = 41,052,429 US dollars per year

4. Average Annual Net Income per Ton of Methanol Converted

Net income per ton of methanol converted = Annual revenue - Annual operating cost - Annual total capital investment = (41,052,429 - 31,745,458.9 - 2,367,308.2) / 10,000 = 694 US dollars

Supplementary Table 1. EXAFS fitting parameters and results at the Ni K-edge of different samples[a]

Sample	Shell	CN	R (Å)	σ^2 (Å^2)	R-factor
Nano-NiO	Ni-O	6.2	2.08	0.00382	0.01123
	Ni-Ni	11.9	2.97	0.00855	
Nano-Vo-NiO	Ni-O	3.6	2.07	0.00161	0.01279
	Ni-Ni	11.4	2.95	0.00930	
Ni Foil	Ni-Ni	12*	2.73	0.00348	0.03243
NiO	Ni-O	6*	2.08	0.00456	0.03026
	Ni-Ni	12*	2.95	0.00595	

[a]CN: coordination number; R: bond distance; σ^2: Debye-Waller factors; R factor: goodness of fit.

*The experimental EXAFS fit of the metal foil by fixing CN as the known crystallographic value.

Supplementary Table 2. The elemental contents in the electrolyte of catalysts after long-term stability tests were analyzed by ICP.

Sample	Ni (mg/L)
Nano-NiO	0.0003
Nano-Vo-NiO	0.0016

Supplementary Table 3. EXAFS fitting parameters and results at the Ni K-edge of Nano-NiO at selected potentials in 1 M KOH[a]

Conditions	Shell	CN	R (Å)	σ^2 (Å^2)	R-factor
OCP	Ni-O	6	2.1	0.00231	0.03018
	Ni-Ni	7.4	2.77	0.01717	
1.2 V	Ni-O	5.5	2.1	0.00871	0.02814
	Ni-Ni	7.0	2.8	0.02609	
1.4 V	Ni-O	5.8	2.07	0.00792	0.06838
	Ni-Ni	7.4	2.86	0.01789	
1.6 V	Ni-O	5.3	2.07	0.00541	0.03220
	Ni-Ni	7.3	2.93	0.04025	

[a]CN: coordination number; R: bond distance; σ^2: Debye-Waller factors; R factor: goodness of fit. The experimental EXAFS fit of the metal foil by fixing CN as the known crystallographic value. The applied potentials are relative to the RHE.

Supplementary Table 4. EXAFS fitting parameters and results at the Ni K-edge of Nano-Vo-NiO at selected potentials in 1 M KOH[a]

Conditions	Shell	CN	R (Å)	σ^2 (Å^2)	R-factor
OCP	Ni-O	4.1	2.06	0.00159	0.00734
	Ni-Ni	6.6	2.78	0.01595	
1.2	Ni-O	4.1	2.05	0.00035	0.01339
	Ni-Ni	6.3	2.80	0.01135	
1.4	Ni-O	4.4	2.05	0.00248	0.20785
	Ni-Ni	6.3	2.85	0.01014	
1.6	Ni-O	3.8	2.00	0.00367	0.10388
	Ni-Ni	5.9	2.88	0.03148	

[a]CN: coordination number; R: bond distance; σ^2: Debye-Waller factors; R factor: goodness of fit. The experimental EXAFS fit of the metal foil by fixing CN as the known crystallographic value. The applied potentials are relative to the RHE.

Supplementary Table 5. A comparison of Nano-Ov-NiO with previously reported catalysts in MOR performance.

Catalysts	Conductive Substrate	Electrolyte	Current density (mA cm^{-2})– Stability time (h)	Refs.
F_{10}-Ni_3N	NF	1 M MeOH 1 M KOH	200–600	[7]
Ni_3FeN-Ru_{buried}	GCE	1 M MeOH 1 M KOH	200–120	[8]
Ni-Mo_2C@C	GCE	1 M MeOH 1 M KOH	200–450	[9]
CeF_3@Ni_3N	CC	1 M MeOH 1 M KOH	300–144	[10]
Pt–Ni_3S_2/CC	GCE	1 M MeOH 1 M KOH	10–36	[11]
Cr-Ni_3S_2	NF	1 M MeOH 1 M KOH	50–30	[12]
$Cr_{0.02}Ni(OH)_{2+\delta}$	NF	1 M MeOH 1 M KOH	60-180	[13]
Ni50Co50-m	GCE	1 M MeOH 1 M KOH	80-30	[14]
NCS/CF	GCE	1 M MeOH 1 M KOH	100-100	[15]
Cr-doped Ni(OH)2	GCE	0.5 M MeOH 1 M KOH	40-15	[16]
NiSnPH@OOH/CC	CC	1 M MeOH 1 M KOH	100-30	[17]
Fe-NF-500	NF	1 M MeOH 1 M KOH	300-40	[18]
Ni-$Bi(OH)_3$/NF	NF	1 M MeOH 1 M KOH	20-250	[19]
NiB-400	GCE	1 M MeOH 1 M KOH	100-24	[20]
CuONS/CF	GCE	1 M MeOH 1 M KOH	20-45	[21]
Mo-NiOOH@ SO_4^{2-}/NF	NF	1 M MeOH 1 M KOH	300-65	[22]
Nano-Ov-NiO	**GCE**	**1 M MeOH 1 M KOH**	**~500-1000**	**This work**

Supplementary Table 6. Plant capital investment worksheet

	electro-catalyzed process ($)
Production process cost	18,768,768.6
Product separation cost	9,384,384.3
Waste treatment device cost	2,252,252.2
Additional utility cost	1,600,284.5
Total installed cost	32,005,689.5
Warehouse cost	1126126.1
Site development cost	2,533,783.7
Additional piping cost	1,266,891.9
Total direct cost	36,932,491.2
Maintenance expenses	3,693,249.1
Field expenses	3,693,249.1
Building and construction expenses	7,386,498.2
Other expenses	3,693,249.1
Total indirect costs	18,466,245.6
Fixed capital investment[b]	55,398,736.8
Land cost	553,987.4
Working capital cost	2,769,936.8
Total capital investment[c]	58,722,661
Equipment life span (years)	15
Total capital investment per year[d]	2,367,308.2

[a]including Total installed cost

[b]Fixed capital investment is the sum of Total direct cost and Total indirect cost.

[c]Total capital investment is the sum of Fixed capital investment, Land cost, and Working capital cost.

[d] Total capital investment is depreciated at a rate of 6%.

Supplementary Table 7. Plant capital investment and operating cost

	electro-catalyzed process ($)
Total capital investment	2,145,713.3
Raw material cost	17,751,237.5
Electricity cost	6,893,726.4
Heat & Steam, cooling water cost	6212933.1
Utility operating cost	13106659.5
Other operating cost	887561.9
Operating Cost[a]	31,745,458.9
Cost per year[b]	33891172.2

[a]Operating cost is the sum of Raw material cost, Utility operating cost, and Other operating cost.

[b]Cost per year is the sum of the total capital investment per year and the operating costs.

Supplementary Table 8. Economic parameters and economic assumptions

Economic parameters	
99.5% methanol ($ per t)[a]	340
KOH price ($ per t)[a]	820
Process water price ($ per t) [a]	0.22
Electricity price ($ per kWh) [a]	0.1
H_2 price ($ per t) [a]	1900
O_2 price ($ per t) [a]	100
potassium formate price ($ per t) [a]	1590
a https://www.spglobal.com/commodityinsights/	
Economic assumptions	
Electrolyzer price ($ per m^2)	10000
Electrocatalyst and membrane price ($ per m^2)	5 % of electrolyzer price
Faradaic efficiency of H_2 (%)	100 %
Faradaic efficiency of methanol electrooxidation (%)	95%
Methanol-to-formate carbon yield for electrocatalysis (%, including separation and recovery, etc.)	95%
Operating time (hours per day/per year)	24/300
Equipment life span (years)	15
Depreciation rate (% per year)	6
Maintenance expenses (% of total direct costs)	10
Working capital (% of fixed capital investment)	5
Operating current density (mA cm^{-2})	300
All the above assumptions are based on previous literatures and realistic conditions.	

Supplementary References

[1] Zhou H, Ren Y, Li Z, Xu M, Wang Y, Ge R, Kong X, Zheng L, Duan H Electrocatalytic upcycling of polyethylene terephthalate to commodity chemicals and H_2 fuel. Nat. Commun. 2021;1(12):4679. http://doi.org/10.1038/s41467-021-25048-x

[2] Wang S, Lin Y, Li Y, Tian Z, Wang Y, Lu Z, Ni B, Jiang K, Yu H, Wang S, Yin H, Chen L Nanoscale high-entropy surface engineering promotes selective glycerol electro-oxidation to glycerate at high current density. Nat. Nanotechnol. 2025;5(20):646-655. http://doi.org/10.1038/s41565-025-01881-9

[3] Wang X, Su Y, Chen J, Yan E H, Xia Q, Wu J, Gong S, Tang M, Yip W S, Mu Y, Yi Y, Wu J, Xu F, Yang X, Zhang X, Dou S, Sun J, Zheng G Revisiting Pt foil catalysts for formamide electrosynthesis achieved at industrial-level current densities. Nat. Commun. 2025;1(16):http://doi.org/10.1038/s41467-025-63313-5

[4] Song M, Wu Y, Zhao Z, Zheng M, Wang C, Lu J Corrosion Engineering of Part-per-million Single Atom $Pt_1/Ni(OH)_2$ Electrocatalyst for PET Upcycling at Ampere-level Current Density. Adv. Mater. 2024;36):2403234. http://doi.org/10.1002/adma.202403234

[5] De Luna P, Hahn C, Higgins D, Jaffer S A, Jaramillo T F, Sargent E H What would it take for renewably powered electrosynthesis to displace petrochemical processes? Science 2019;6438(364):http://doi.org/10.1126/science.aav3506

[6] Kim H J, Kim Y, Lee D, Kim J-R, Chae H-J, Jeong S-Y, Kim B-S, Lee J, Huber G W, Byun J, Kim S, Han J Coproducing Value-Added Chemicals and Hydrogen with Electrocatalytic Glycerol Oxidation Technology: Experimental and Techno-Economic Investigations. ACS Sustainable Chem. Eng. 2017;8(5):6626-6634. http://doi.org/10.1021/acssuschemeng.7b00868

[7] Qin H, Li J, Lin G, Yuan K, Yang H, Ye Y, Jin T, Cheng F, Jiao L Tuning Surface Coordination Environment of Ni3N by Fluorine Modification for Efficient Methanol Electrooxidation Assisted Hydrogen Evolution. Adv. Mater. 2025;33(37):2507573. http://doi.org/10.1002/adma.202507573

[8] Lin Y, Geng B, Zheng R, Chen W, Zhao J, Liu H, Qi Z, Yu Z, Xu K, Liu X, Yang L, Shan L, Song L Optimizing surface active sites via burying single atom into subsurface lattice for boosted methanol electrooxidation. Nat. Commun. 2025;1(16):286. http://doi.org/10.1038/s41467-024-55615-x

[9] Lin G, Qin H, Cao X, Cheng F, Jiao L, Chen J Regulation of Relay Catalytic Mechanism for Efficient Methanol Oxidation Reaction. Angew. Chem. Int. Ed. 2025;42(64):e202506215. http://doi.org/10.1002/anie.202506215

[10] Deng K, Liu X, Liu P, Lv X, Tian W, Ji J Enhanced Adsorption Kinetics and Capacity of a Stable CeF_3@Ni_3N Heterostructure for Methanol Electro-Reforming Coupled with Hydrogen Production. Angew. Chem. Int. Ed. 2025;4(64):e202416763. http://doi.org/10.1002/anie.202416763

[11] Zhao Q, Zhao B, Long X, Feng R, Shakouri M, Paterson A, Xiao Q, Zhang Y, Fu X-Z, Luo J-L Interfacial Electronic Modulation of Dual-Monodispersed Pt–Ni_3S_2 as Efficacious Bi-Functional Electrocatalysts for Concurrent H2 Evolution and Methanol Selective Oxidation. Nano-micro Lett. 2024;1(16):80. http://doi.org/10.1007/s40820-023-01282-4

[12] Saj A A, Bhunia K, Sajeev A, Jae Kim S Doping-mediated interface engineered Ni_3S_2: Economically viable electrochemical methanol-mediated water splitting. Chem. Eng. J. 2024;7(499):156284. http://doi.org/10.1016/j.cej.2024.156284

[13] Qin H, Ye Y, Lin G, Zhang J, Jia W, Xia W, Jiao L Regulating the Electrochemical Microenvironment of Ni(OH)2 by Cr Doping for Highly Efficient Methanol Electrooxidation. ACS Catal. 2024;21(14):16234-16244. http://doi.org/10.1021/acscatal.4c05729

[14] Qi Y, Zhu Y, Jiang H, Li C Promoting electrocatalytic oxidation of methanol to formate through interfacial interaction in NiMo oxide-CoMo oxide mixture-derived catalysts. Chin. J. Catal. 2024;56):139-149. http://doi.org/10.1016/s1872-2067(23)64565-6

[15] Li J, Yu H, Chi J, Luo X, Li T, Shao Z An efficient $NiCoSe_4$/NiCo-LDH/CF catalyst for the co-production of value-

added formate and hydrogen via selective methanol electro-oxidation. J. Mater. Chem. A 2024;38(12):25791-25800. http://doi.org/10.1039/d4ta04581e
[16] Fan Y, Yang X, Wei E, Dong Y, Gao H, Luo X, Yang W Promoted electro-oxidation kinetics in chromium-doped α-$Ni(OH)_2$ nanosheets for efficient selective conversion of methanol to formate. Appl. Catal., B 2024;3(345):123716. http://doi.org/10.1016/j.apcatb.2024.123716
[17] Shao J, Fang Y, Wu X, Abdullah M I, Tao Y Unraveling the role of NiSnPH@OOH/CC perovskite hydroxide for efficient electrocatalytic oxidation of methanol to formate. Nano Research 2023;4(17):2388-2399. http://doi.org/10.1007/s12274-023-6078-z
[18] Hao Y, Yu D, Zhu S, Kuo C-H, Chang Y-M, Wang L, Chen H-Y, Shao M, Peng S Methanol upgrading coupled with hydrogen product at large current density promoted by strong interfacial interactions. Energy Environ. Sci. 2023;3(16):1100-1110. http://doi.org/10.1039/d2ee03936b
[19] Hao S, Cong M, Xu H, Ding X, Gao Y Bismuth-Based Electrocatalysts for Identical Value-Added Formic Acid Through Coupling CO_2 Reduction and Methanol Oxidation. Small 2023;21(2307741. http://doi.org/10.1002/smll.202307741
[20] Qi Y, Zhang Y, Yang L, Zhao Y, Zhu Y, Jiang H, Li C Insights into the activity of nickel boride/nickel heterostructures for efficient methanol electrooxidation. Nat. Commun. 2022;1(13):4602. http://doi.org/10.1038/s41467-022-32443-5
[21] Wei X, Li Y, Chen L, Shi J Formic Acid Electro-Synthesis by Concurrent Cathodic CO_2 Reduction and Anodic CH_3OH Oxidation. Angew. Chem. Int. Ed. 2020;6(60):3148-3155. http://doi.org/10.1002/anie.202012066
[22] Chen T, Chen K, Zong Q, Li Z, Huang L In Situ Fabrication of Sulfate-Grafted Mo-Doped NiOOH for Electrocatalytic Methanol Oxidation Coupled With Hydrogen Production at Industrial-Level Current Density. Rare Met. 2025;45):e70001. http://doi.org/10.1002/rar2.70001